

Diss. ETH No. 20799

^{220}Rn in Groundwater and Soil Gas

A dissertation submitted to
ETH ZURICH

for the degree of
DOCTOR OF SCIENCES

presented by
STEPHAN CASPAR HUXOL
Diplom Hydrologe, University of Freiburg, Germany
born 19.02.1981
citizen of Germany

accepted on the recommendation of
Prof. Dr. Rolf Kipfer, examiner
Dr. Eduard Hoehn, co-examiner
Dr. Heinz Surbeck, co-examiner
Prof. Dr. Dani Or, co-examiner

2012

Chapter 3 has been published as:

Huxol, S., Brennwald, M. S., Hoehn, E. and Kipfer, R. (2012). On the fate of ^{220}Rn in soil material in dependence of water content: Implications from field and laboratory experiments. *Chemical Geology*, 298-299:116-122.

DOI: <http://dx.doi.org/10.1016/j.chemgeo.2012.01.002>.

Chapter 4 has been published as:

Huxol, S., Brennwald, M. S. and Kipfer, R. (2013). Processes controlling ^{220}Rn concentrations in the gas and water phases of porous media. *Chemical Geology*, 335:87-92. DOI: <http://dx.doi.org/10.1016/j.chemgeo.2012.10.049>.

Chapter 5 is in preparation for publication in *Environmental Science and Technology*:

Huxol, S., Brennwald, M. S., Henneberger, R. and Kipfer, R. The different behavior of ^{220}Rn and ^{222}Rn in soil gas transport processes and its application.

Acknowledgments

First of all, I would like to thank my referees of my dissertation *Rolf Kipfer*, *Dani Or*, *Eduard Hoehn* and *Heinz Surbeck*. Edi's instructions to the radon measurement techniques and his valuable advices in the first years of the thesis helped a lot. Heinz is thanked for sharing his great experience with radionuclides in water. Dani is thanked for readily and spontaneously taking over the job as co-examiner. Most notably, Roki's enthusiastic support, his talent to motivate and to bring the important thoughts on the point, and his believe in the relevance of the topic ("Do you think, we fly to the moon to invent teflon-pans?" greatly contributed to the completion of this thesis.

A special thank goes to *Evelin Vogler*, who did a great job during her master thesis and produced the results that turned the scope of the thesis into the right direction. *Matthias Brennwald* is thanked for fruitful discussions and his help whenever I was fighting with some MatLab-code. I also like to thank *Rolf Mahrer* from Rothenbrunnen, who provided me with the manganese sand and was on the spot every time when I needed a new delivery. *Marian Furjak* need to be thanked for the gamma-analysis of all the sands and soils I brought him. *Ralf Kägi* is thanked for producing the electron microscope pictures of the substrates I used in my experiments. A great thank you goes to *Andreas Raffener* and *Peter Gäumann*, who gave technical support and constructed all the laboratory facilities (spray chamber, water pumps, sandbox, tank...), which I only sketched with a few lines on paper. The Soil and Terrestrial Environmental Physics Group (STEP) at ETH and especially *Hans Wunderli* and *Dani Breitenstein* are thanked for their advice and hosting me in their soil physics laboratory.

It was a great pleasure to be part of the Environmental Isotopes Group at Eawag, thank you for creating a comfortable and relaxing working atmosphere: *Helena Amaral*, *Yvonne Scheidegger*, *Lars Mächler*, *Simon Figura*, *Yama Tomonaga* (thank you for taking care of our daily caffeine dose in appropriate quality!), *Ryan North*, *Lina Tyroller*, *Ola Kwiecien*, *Nadia Vogel* and *David Livingstone*.

Finally, I want to thank my friends and family, especially *Johanna Huxol* for enduring all my ups and downs, and our two wonderful boys, who remind me every day, what really is important.

Contents

1	Introduction	1
1.1	Introduction and scope of work	1
1.2	Outline	2
2	Scientific background	5
2.1	History and health aspects	5
2.1.1	The discovery of radon isotopes	5
2.1.2	Radon as health hazard	6
2.2	The natural radioactive noble gas radon	6
2.2.1	Emanation	8
2.2.2	Dependence of the emanation coefficient on parameters specific to the solid material	10
2.3	Geophysical and geochemical behavior of the radon isotope pre- cursors	12
2.4	The different half-lives of the radon isotopes and the potential re- sulting application of ^{220}Rn as a natural tracer	13
2.5	The radon monitor “RAD7”	14
2.6	The natural ^{220}Rn sources used in the laboratory experiments	15
3	On the fate of ^{220}Rn under changing water contents	19
3.1	Introduction	19
3.2	Continuous measurements of ^{220}Rn and ^{222}Rn in a natural soil . . .	22
3.3	Conceptual model of ^{220}Rn release from soil grains to soil gas	24
3.4	Experimental setup to test the conceptual model	26
3.5	Results and discussion	27
3.5.1	Influence of water content	27
3.5.2	Influence of turbulence	28
3.5.3	Implications of the results for ^{220}Rn -in-water measurements	29
3.6	Summary and conclusion	30
3.7	Annex 1: ^{220}Rn -analysis in water: Method	31

3.8	Annex 2: ^{220}Rn -analysis in water: Results	33
3.9	Annex 3: Emanation of ^{220}Rn from iron and manganese precipitates	34
4	Processes controlling ^{220}Rn concentrations in the gas and water phases of porous media	37
4.1	Introduction	38
4.2	Material and methods	39
4.2.1	Sand	40
4.2.2	Sandbox	41
4.2.3	Tank	42
4.2.4	Experimental work	43
4.3	Results and discussion	44
4.3.1	Hysteresis of ^{220}Rn in the gas phase	44
4.3.2	Dependence of ^{220}Rn emanation on fl w velocity	45
4.4	Summary and conclusion	48
4.5	Annex 1: Sand properties	49
4.5.1	Emanation coefficient	49
4.5.2	Soil water characteristic curve	49
5	The different behavior of ^{220}Rn and ^{222}Rn in soil gas transport pro- cesses and its application	51
5.1	Introduction	52
5.2	Material and methods	53
5.2.1	Laboratory measurements	53
5.2.2	Field measurements	56
5.3	Results and discussion	57
5.3.1	A. Diffusion	57
5.3.2	B. Advection	59
5.3.3	Field results	61
6	Synthesis and outlook	65
	Bibliography	67
	Corrigendum	77
	Curriculum Vitae	79

Summary

This thesis focuses on the use of the short-lived radon isotope ^{220}Rn (half-life 55.6 s) as environmental tracer in groundwater and soil gas. Radon is a natural radioactive noble gas and its isotopes are produced by alpha decay of their precursor radium isotopes. From radium bearing minerals in the subsurface, radon isotopes are released to the environment, i.e. groundwater and soil gas.

The longer-lived ^{222}Rn (half-life 3.8 d) is used for decades as environmental tracer in subsurface fluids. The short lived ^{220}Rn , however, gained much less interest in environmental sciences and was only in soil gas rarely applied as a tracer. The initial motivation of this thesis, therefore, focused on the determination and use of ^{220}Rn as a tracer in aquatic systems. Here, ^{220}Rn could be used to study small scale processes and as a co-tracer for the long-lived ^{222}Rn in aquatic systems. In order to enable the use of ^{220}Rn as a tracer in aquatic systems, the sampling and measurement technique of ^{220}Rn -in-water concentrations had to be optimized. As the used radon isotope detector is an radon-in-air detection system, the water to be analyzed has to be degassed before analysis. By testing and modifying different degassing devices and by adding an additional air loop with an adjustable air pump to the detection system, the travel time of water and air between sampling and radon analysis was reduced. Consequently, the feasibility of ^{220}Rn -in-water detection was proven in laboratory experiments. When the system was applied to the field to sample natural groundwater, however, significant concentrations ^{220}Rn were measured only in one special case, in which water was sampled directly from a pipe with inner coatings of ^{220}Rn -producing material. In all other cases, no ^{220}Rn was detected in water.

To find out, why ^{220}Rn cannot be detected in natural groundwaters, the ^{220}Rn behavior in the gaseous phase in porous media was studied in the field and laboratory. As ^{220}Rn is known to be ubiquitous in soil gas, a soil gas measurement campaign in a vertical soil profile near a river was initiated. During this campaign, the groundwater table at the field site rose as a result of elevated river discharge. From the moment when the groundwater table reached the lowermost sampling point, the ^{220}Rn concentration in this depth dropped to zero, while ^{222}Rn was still detectable. This result indicated that the water content of soils plays a major role in the availability of ^{220}Rn in soil gas.

Laboratory experiments revealed that, due to the short half-life of ^{220}Rn , water acts as barrier in which ^{220}Rn decays before passing it diffusively. Hence, under partially saturated conditions, water film hinder the release of ^{220}Rn from the grains and water menisci limit the migration of ^{220}Rn through the pore space. Un-

der saturated conditions, ^{220}Rn decays in immobile water layers around the grains and therefore does not reach the moving water phase in natural groundwaters. Consequently, in saturated porous media, ^{220}Rn can not be detected under common natural environmental conditions by common sampling techniques. However, targeted laboratory experiments, in which uncommonly high water flow velocities through saturated porous media were induced, show that the applied shear stress of the fast flowing water can disturb and reduce the thickness of the constraining water layers. These extreme and unnatural conditions stimulate the ^{220}Rn release from the grains to the flowing water. Similar stimulation of the ^{220}Rn -release due to advective gas movements was found under unsaturated conditions, too.

Moreover, regarding gas transport processes, the results of the thesis show that, due to its short half-life, the ^{220}Rn concentrations in the gas phase of porous media are much less affected by changes of the diffusive and advective transport conditions compared to the ^{222}Rn concentrations. Hence, the ^{220}Rn concentration are less susceptible to movements or mixing of gas, which in the field often make the interpretation of ^{222}Rn -in-soil gas concentrations difficult and its use as a tracer ambiguous. The thesis therefore proposes and shows for the first time, how by the combined determination of ^{222}Rn and ^{220}Rn the relevant soil gas transport processes can be identified

In summary, this thesis addresses the question and yields insights, why ^{220}Rn is ubiquitous in soil gas but not detectable under saturated conditions in common natural settings and with common sampling techniques. Therefore, ^{220}Rn commonly cannot be applied as an environmental tracer in aquatic systems. In soil gas, however, it is concluded that the potential of ^{220}Rn as environmental tracer is not fully developed and its exploration should be enforced in the future.

Zusammenfassung

Diese Arbeit beschreibt die Anwendung des kurzlebigen Radonisotopes ^{220}Rn (Halbwertszeit 55.6 s) als natürlichen Tracer in Grundwasser und Bodengas. Radon ist ein natürliches radioaktives Edelgas. Radonisotope entstehen durch Alpha-zerfall der jeweiligen Radiumvorgängerisotope. Aus radiumhaltigen Mineralien werden die Radonisotope in das Grundwasser und Bodengas freigesetzt.

Schon seit Jahrzehnten wird das langlebige Radonisotope ^{222}Rn (Halbwertszeit 3.8 d) in Grundwasser und Bodengas als Tracer verwendet. Das kurzlebige ^{220}Rn dagegen fand viel weniger Beachtung in den Umweltwissenschaften und wird nur selten und ausschliesslich im Bodengas als Tracer verwendet. Die anfängliche Motivation für diese Arbeit war deshalb die Bestimmung und Anwendung von ^{220}Rn als Tracer in aquatischen Systemen. Um dies zu ermöglichen, musste zuerst die Probenahme und die Analysemethode verbessert werden. Da der benutzte Radondetektor die Radonisotope in der Gasphase misst, muss das zu analysierende Wasser zuerst entgast werden. Es wurden verschiedene Systeme zur Entgasung von Wasser getestet und modifiziert. Unter anderem, indem ein zusätzlicher Luftkreislauf mit einer regelbaren Membranpumpe zwischen Radondetektor und Entgasungssystem installiert wurde, konnten die Verweilzeiten von Wasser und Luft zwischen der Beprobung und der Analyse verringert werden. So konnte letztendlich die Machbarkeit der Messung von ^{220}Rn in Wasser in Laborversuchen gezeigt werden. Im Feld wurden mit dem entwickelten Messsystem verschiedene Grundwässer auf ^{220}Rn -Konzentrationen getestet. Allerdings konnte, mit einer Ausnahme, in der das Wasser direkt aus einem Rohr mit ^{220}Rn produzierenden Ablagerungen strömte, kein ^{220}Rn gefunden werden konnte.

Um herauszufinden warum ^{220}Rn in natürlichen Grundwässern nicht nachgewiesen werden kann, wurde das Auftreten von ^{220}Rn in der Gasphase von porösen Medien im Feld und Labor untersucht. Aus der Literatur ist bekannt, dass ^{220}Rn im Bodengas allgegenwärtig ist. Daher wurde ^{220}Rn in einem Bodengasprofil in der Nähe eines Flusses kontinuierlich bestimmt. Infolge eines Hochwassers während dieser Messkampagne stieg der Grundwasserspiegel so hoch, dass die unterste Messtiefe geflutet wurde. Bei Sättigung ging die ^{220}Rn -Konzentration gegen Null, während sich die ^{222}Rn -Konzentration nur geringfügig änderte. Diese Resultate zeigten, dass das Auftreten von ^{220}Rn stark durch den Bodenwassergehalt bestimmt wird.

Entsprechende Laborexperimente zeigten, dass Wasser als Barriere wirkt, welche ^{220}Rn aufgrund seiner kurzen Halbwertszeit nicht passieren kann. Das heisst, unter teilweise gesättigten Bedingungen behindern Wasserfilm die Freisetzung

von ^{220}Rn aus den Körnern. Gleichzeitig schränken Wassermenisken zwischen den Körnern die Mobilität von ^{220}Rn im Porenraum ein. Unter gesättigten Bedingungen zerfällt ^{220}Rn in immobilen Wasserschichten am Rande des durchflossenen Porenraumes und erreicht daher nicht den beweglichen Teil des Grundwassers. Daher kann ^{220}Rn in natürlichen Grundwassersystemen unter “normalen” Bedingungen nicht gemessen werden.

Zielgerichtete Laborexperimente, in denen Wasser aussergewöhnlich schnell durch ein poröses Medium bewegt wurde, zeigen allerdings, dass die unbewegten Wasserschichten durch Scherkräfte gestört und in ihrer Dicke verringert werden können. Dies bewirkt, dass ^{220}Rn das advektiv bewegte Wasser erreicht und entsprechend detektiert werden kann. Der gleiche Effekt, das heisst erhöhte ^{220}Rn -Konzentrationen durch erhöhte advektive Gasflüsse, tritt auch unter ungesättigten Bedingungen auf.

Die Arbeit zeigt ausserdem, dass die ^{220}Rn -Konzentrationen im Bodengas wegen der kurzen Halbwertszeit viel weniger stark als die ^{222}Rn -Konzentrationen durch Transportprozesse beeinflusst werden. Daher sind die ^{220}Rn -Konzentrationen viel weniger anfällig auf advektive Gasbewegungen oder Mischungsvorgänge, welche die Interpretation von ^{222}Rn -Konzentrationen im Bodengas häufig erschweren und uneindeutig machen. Die vorliegende Arbeit zeigt erstmalig, wie durch die gemeinsame Bestimmung von ^{222}Rn und ^{220}Rn in der Gasphase eines Bodenprofils die relevanten Transportprozesse identifiziert werden können.

Zusammenfassend liefert diese Arbeit eine schlüssige konzeptionelle Vorstellung, warum ^{220}Rn , im Gegensatz zu ^{222}Rn , ausschliesslich im Bodengas, aber nicht unter natürlichen Bedingungen und mit herkömmlichen Probenahmetechniken im Grundwasser zu finden ist. Daher kann ^{220}Rn nicht als Tracer in aquatische Systemen verwendet werden. Im Bodengas ist die Anwendung von ^{220}Rn als Tracer jedoch noch kaum entwickelt, weshalb die Forschung in diesem Bereich in Zukunft verstärkt werden sollte und sich deshalb als zukünftiges Forschungsfeld anbietet.

Chapter 1

Introduction

1.1 Introduction and scope of work

Radon is a natural radioactive noble gas. Its isotopes are generated in the subsurface by radioactive decay of radium isotopes. As a noble gas, radon isotope concentrations in subsurface fluid have become a powerful tool to analyze transport processes in groundwater and soil gas. Corresponding to their different half-lives, the radon isotopes are used in the environmental systems at very different scales.

In aquatic systems, concentrations of the long-lived ^{222}Rn (half-life 3.82 d) in groundwater are used to study groundwater inflow into surface water bodies as oceans (Cable et al., 1996; Santos et al., 2009), lakes (Kluge et al., 2007; Dimova and Burnett, 2011a) or rivers (Mullinger et al., 2007; Peterson et al., 2010). Also the infiltration of surface water into groundwater bodies is studied. By analyzing the ingrowth of ^{222}Rn concentrations along a groundwater flow path, the groundwater age of freshly infiltrate surface water can be determined (Hoehn and von Gunten, 1989; Hoehn and Cirpka, 2006).

The exchange of soil gas with the atmosphere was studied by analyzing exhalations of ^{222}Rn on the regional scale (Schmidt et al., 1996; Hirsch, 2007). On the local scale, the structure of the lower atmosphere was studied by analyzing ^{222}Rn concentrations (Sesana et al., 1998; Fujiyoshi et al., 2010). Atmospheric concentrations of the short-lived isotope ^{220}Rn (half-life 55.6 sec) near the soil surface were used to study small scale micrometeorological fluxes (Lehmann et al., 1999, 2001).

The aim of this thesis was to evaluate the use of ^{220}Rn concentrations in groundwater as a small scale tracer. Being able to determine ^{220}Rn in groundwater, ^{220}Rn concentrations could be used to study small scale processes or to act as a co-tracer with the well-established ^{222}Rn , e.g. to enhance the groundwater age dating with ^{222}Rn . However, in the light of its very short half-life, the

measurement of ^{220}Rn from groundwater samples is experimentally challenging. Therefore, the first target of this thesis was to optimize the sampling procedure and to develop a robust and reliable measurement protocol that allows to determine the ^{220}Rn -in-water concentrations.

In addition, ^{222}Rn and ^{220}Rn have different half-lives and are part of different decay series. Therefore, the release of the different radon isotopes from solid soil grains to the surrounding fluid (“emanation”) is expected to be different. While for ^{222}Rn the emanation process and the factors that influence the emanation are principally known (Bossus, 1984; Rama and Moore, 1984; Nazaroff, 1992), for ^{220}Rn the emanation behavior still has to be characterized.

Having the knowledge about the emanation and the measurement technique for ^{220}Rn -in-water at hand, ^{220}Rn concentrations in groundwater are a promising tool to trace small scale and short time processes as e.g. upwelling and downwelling in riverbeds. Moreover, the groundwater age-dating method with ^{222}Rn is susceptible to changes of the ^{222}Rn emanation along the groundwater flow path, and to mixing with water of different age. The ^{220}Rn concentrations, however, due to the short half-life of ^{220}Rn , reflect only the local conditions. Therefore, the ^{220}Rn concentrations are not affected by mixing with water of different age, but only by changes in the emanation. Hence, by the combined determination of the ^{220}Rn and ^{222}Rn concentration in groundwater, mixing processes or changes in the emanation could be identified and the reliability of the groundwater age-dating method would be greatly enhanced.

This thesis provides the fundamental research for the use of ^{220}Rn as a tracer in subsurface fluid as groundwater and soil gas. This includes the development of detection systems to analyze and study ^{220}Rn in the subsurface. Results of the application of these systems are presented and the limitations and benefit of the use of ^{220}Rn as a tracer in subsurface fluid are discussed. The following section describes the structure of this thesis.

1.2 Outline

Scientific background (Chapter 2): A general overview about the radioactive noble gas radon and its natural occurring isotopes is given. The emanation process is described and general factors that influence the emanation of radon isotopes from the solid grains to the environment are discussed. The chapter also provides some background information about the different geochemical and geophysical histories of ^{220}Rn and ^{222}Rn as consequence of belonging to different decay series. Finally, the functionality and advantages of the used radon detector system are described shortly and the used ^{220}Rn sources are introduced.

On the fate of ^{220}Rn in dependence of water content: Implications from field and laboratory experiments (Chapter 3): With a detection system that was proven to detect ^{220}Rn in water under laboratory conditions, 10 different groundwater systems from all over Switzerland were studied whether they contain ^{220}Rn . But only in one specific case ^{220}Rn could be found. A field campaign targeting the ^{220}Rn concentrations in soil gas revealed the soil water content as a major driving factor on the ^{220}Rn concentrations. A conceptual model was developed that explains the absence of ^{220}Rn under saturated conditions. Hereby the slow diffusion of ^{220}Rn through water layers around and water menisci between the soil grains limits the emanation and mobility of ^{220}Rn . The model is tested and validated with laboratory experiments using monazite pebbles and manganese sand as sources of ^{220}Rn . This chapter has been published in Chemical Geology (Huxol et al., 2012).

Processes controlling ^{220}Rn concentrations in the gas and water phases of porous media (Chapter 4): The results of laboratory experiments with a sandbox which allows to simulate water table fluctuations and with a tank filled with saturated sand to simulate groundwater flow are presented. The results of the sandbox revealed that a changing water content causes the development of water menisci between the sand grains. These water menisci strongly delimit the migration range of ^{220}Rn through the porous media and therefore reduce the ^{220}Rn concentration in the gas phase. Under saturated conditions, however, immobile water film around the grains strongly inhibit the ^{220}Rn release. High water flow velocities can disturb these water layers by the induced shear stress. High water flow velocities therefore increase the release of ^{220}Rn from the grains. This chapter has been published in Chemical Geology (Huxol et al., 2013).

The different behavior of ^{220}Rn and ^{222}Rn in soil gas transport processes and its application (Chapter 5): The behavior of ^{220}Rn and ^{222}Rn in the gas phase was studied in the sandbox by changing the conditions for diffusive and advective gas transport. The results show that, in contrast to the ^{222}Rn concentrations, the ^{220}Rn concentrations in the gas phase do not change when ever (1) the connection to the atmosphere is blocked, or (2) fresh air is introduced advectively through the sandbox. Hence, the ^{220}Rn concentrations are much less influenced by changes of gas transport than the ^{222}Rn concentrations. By adapting the gained insights from the laboratory experiments to the field it is shown that the combined analysis of ^{220}Rn and ^{222}Rn in soil gas strengthens the interpretation of measurements of reactive soil gases. This chapter is in preparation for publication in Environmental Science and Technology.

Conclusions and outlook (Chapter 6): This chapter summarizes the most important finding of the thesis and gives an outlook for possible future research and applications of ^{220}Rn in environmental studies.

Chapter 2

Scientific background

2.1 History and health aspects

2.1.1 The discovery of radon isotopes

The turn to the 20th century was an exciting time for scientific discoveries and technical inventions. After the discovery of the radioactivity by Antoine Becquerel in 1896, and the detection of the first radioactive elements by Pierre and Marie Curie, radon was discovered as the fifth radioactive element contemporaneously by Ernst Dorn, Ernest Rutherford and André-Louis Debierne in 1900. Dorn discovered that the “induced radioactivity”, which was generated by the decay of radium, was related to a radioactive gas that Dorn called “Emanation” (Dorn, 1900). Later in 1900, Rutherford discovered that also thorium generates such gaseous “Emanation” (Rutherford, 1900), while also Debierne discovered a gas, generated from actinium (Debierne, 1900). Depending on the source substance, the gases were called “radium-emanation”, “thorium-emanation” and “actinium-emanation”. As the existence of isotopes was unknown, they were all referred as individual elements.

In 1904, the discoverer of the noble gases Sir William Ramsay suggested that also the “emanations” might be noble gases (Ramsay and Collie, 1904). In 1910, Sir William Ramsay and Robert Whytlaw-Gray isolated radon, determined its density and found it to be the heaviest known gas (Ramsay and Gray, 1910). Since 1923, after the discovery of the isotopes, all emanations were identified as isotopes of the radioactive noble gas radon. However, the historic trivial names “radon” (^{222}Rn), “thoron” (^{220}Rn) and “actinon” (^{219}Rn) are sometimes still in use.

2.1.2 Radon as health hazard

Radon gas is responsible for the majority of the public exposure to ionizing radiation and is therefore considered to be a health hazard when being inhaled (Committee on the Biological Effects of Ionizing Radiations, National Research Council, 1988). Initial concerns focused on the health risk of underground miners exploiting uranium and other ores. Already in the 16th century, Paracelsus reported about the high incidence of fatal respiratory diseases among eastern Europe miners. Later, in the 19th century, Härting and Hesse (1879) identified the “Bergkrankheit” (mountain disease) as lung cancer. In the first half of the 20th century, studies in Germany and the United States gradually revealed that the inhalation of radon and the radon decay products caused this health risk. Hence, it was found that the daughter products of radon are solid and can adsorb to the airways and the lung, increasing the risk of lung cancer (Committee on the Biological Effects of Ionizing Radiations, National Research Council, 1988).

In the second half of the 20th century, concerns of health risk due to “indoor radon” emerged. Depending on the underlying geology, radon that originates from the soils and rocks was found in increased concentration in the cellars and first floor of houses. Also smoking cigarettes exposes the smokers lung to radon isotopes (Nazaroff, 1992).

However, radon is also suggested to ease auto-immune diseases such as arthritis, but also asthma and dermatitis. People seeking relief from such health problems expose themselves therefore for limited periods of time to radon containing air and water in so-called “health-mines” and “radon water baths”. The health effect on people inhaling radon in low doses and taking baths in water enriched with radon is believed to invigorate and energize the cells. The beneficial of this practices, however, is only indicated, but not statistically proven by scientific studies (Franke et al., 2000; Nagy et al., 2009).

2.2 The natural radioactive noble gas radon

Like the other noble gases (helium, neon, argon, krypton and xenon), the outer shell of valence electrons of radon is considered to be “complete”. Therefore, radon has only little tendency to participate in chemical reactions and is not metabolized by microorganisms. This makes radon an ideal trace gas to study physical processes. Being radioactive, radon can be used as a dating tool, too.

The decay of a number N of radioactive atoms is a stochastic process, described by

$$N(t) = N_0 e^{-\lambda t} \quad (2.1)$$

whereas N_0 is the initial number of radioactive atoms, λ is the isotope specific

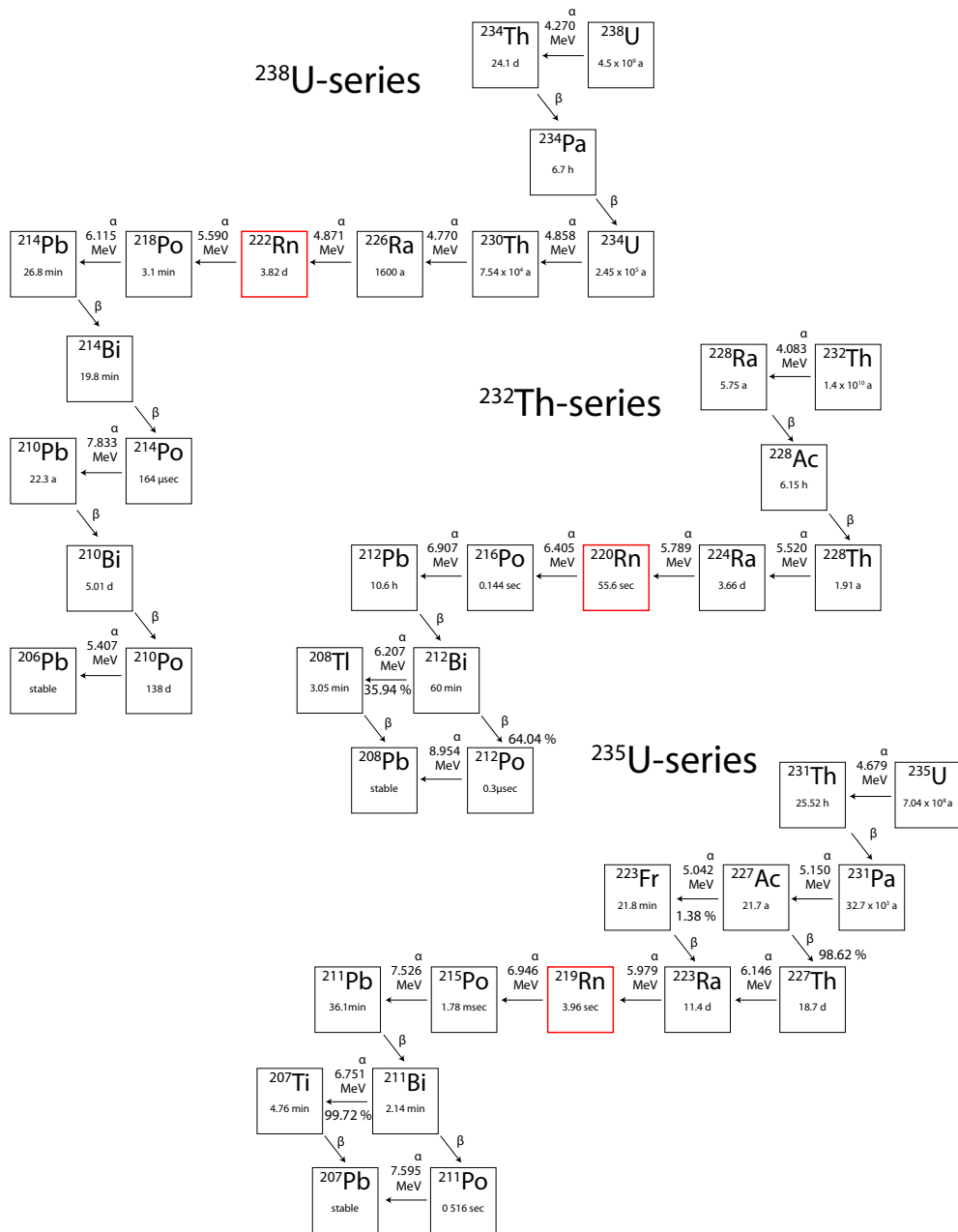


Figure 2.1: ^{238}U , ^{232}Th and ^{235}U decay-series. Half-lives are noted in the isotopes box. Horizontal arrows indicate alpha decay, diagonal arrows indicate beta decay, numbers above arrows the specific alpha decay energy (reproduced from Ekström and Firestone, 2004, and Magill and Galy, 2005).

decay constant, and t is the time. The half-life of radioactive isotopes $t_{1/2}$ describes the time, after which half of the initial number of atoms N_0 is decayed, i.e. $N(t)/N_0 = 0.5$. After equation 2.1, the half-life is related to the isotope specific decay constant λ by $t_{1/2} = \ln(2)/\lambda$.

Radioactive isotopes disintegrate by alpha, beta or gamma decay. In alpha decay, an alpha particle, consisting of two neutrons and two protons bound together as a He nucleus, is ejected. The decaying isotope is transformed into a daughter isotope with mass number reduction of 4 and atomic number reduction of 2. The energies of alpha decay are specific for each decaying isotope (Ivanovich and Harmon, 1982). In beta decay, a negative or positive beta particle, i.e. an electron or positron, is emitted from the decaying isotope. Hence, the atomic number changes by ± 1 , whereas the mass number remains the same. Unlike alpha particles, emitted beta particles do not have a discrete energy, but are distributed over a range from zero to an isotope-characteristic maximal value (Ivanovich and Harmon, 1982). Daughter isotopes, which are generated from alpha or beta decay are often in an excited state and emit electromagnetic radiation, namely gamma rays. In gamma decay, a photon is emitted. Therefore, only the energy of the isotope changes, but neither the mass number nor the atomic number. (Ivanovich and Harmon, 1982).

Radon has three natural occurring isotopes. The longest lived isotope is ^{222}Rn with a half-life of 3.82 d, followed by ^{220}Rn with a half-life of 55.6 s. With a half-life of only 3.96 s, ^{219}Rn is the shortest lived natural radon isotope.

The three natural radon isotopes are part of three different natural decay series: ^{222}Rn is part of the ^{238}U -series, ^{220}Rn of the ^{232}Th -series and ^{219}Rn of the ^{235}U -series (Figure 2.1). All radon isotopes are generated by alpha decay of their respective radium precursor and decay to their respective polonium daughter. However, as radon is the only gaseous element in the decay series, it has an enhanced mobility. Hence, in comparison to the other elements, radon isotopes can get released from the solid material where they were generated and have the tendency to move by diffusion and convection.

Due to the low abundance of its parent isotope ^{235}U (only 0.7 % of earth's total uranium; Binder, 1999) and due to its very short half-life, ^{219}Rn plays only a minor role in the environment and is therefore not discussed further in this thesis.

2.2.1 Emanation

In the subsurface, radon is continuously produced by the alpha decay of radium. At the disintegration of a radium isotope, simultaneously radon is generated and an alpha particle is emitted. Due to recoil, the alpha particle and the newly generated radon isotope move away from their place of formation. The recoil length of the radon isotope hereby depends on the isotope specific recoil energy and the

density of the matter that the newly generated radon isotope has to cross (for typical values see Table 3.2). However, if the decaying radium isotopes are located near a grain's surface, i.e. the grain's border is in the range of the recoil length, and the generated radon is recoiled into the direction of the grain's border, a part of the radon isotopes have chance to get released from the solid grains and reach the pore space.

The process of getting released from the solid material to the air or water filled pore space by recoil and diffusion is called “emanation”. Depending on the detailed emanation mechanistics, distinction is made between “direct”, “indirect” and “diffusive” emanation (Tanner, 1980).

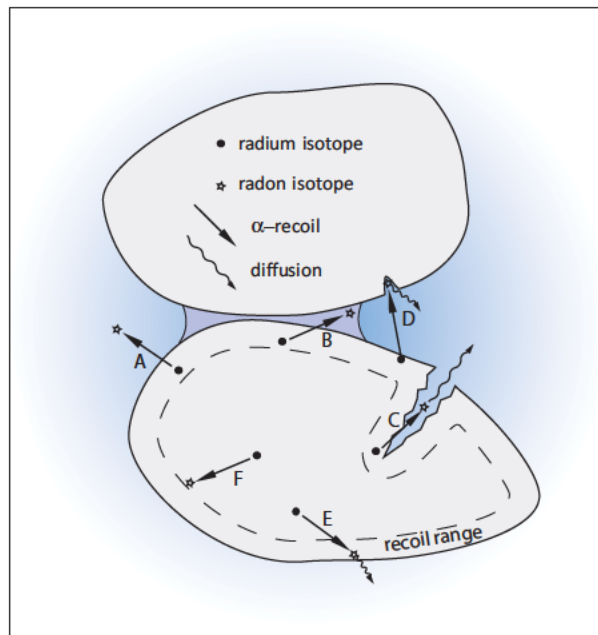


Figure 2.2: Concept of emanation from minerals towards soil gas and water. “A” describes direct emanation into pore space, “B”: direct emanation to water meniscus, “C”: recoil in to intra-granular pore with subsequent diffusion into pore space, “D”: indirect emanation with implanting into adjacent grain with subsequent diffusion back to the pore space, “E”: emanation by diffusion out of the grain, “F” describes the generation of radon without emanation. Dashed line indicates the boundary for radon isotopes to escape from the solid. Symbols greatly exceed atomic dimensions (Reproduced from Tanner, 1980).

Direct emanation The recoil length and direction of directly emanated radon isotopes is such that the generated radon isotopes are ejected from the solid material to the pore space. In the pore space, the radon isotopes are stopped and terminate their recoil path (Figure 2.2 A, B, C).

Indirect emanation The recoil length of indirectly emanated radon isotopes exceed the width of the pore space. The generated radon isotopes are therefore implanted into the wall of adjacent grains where they form “pockets”. From these pockets, radon isotopes can diffuse back into the pore space, as the solid material is structurally weakened by the collision energy (Figure 2.2 D).

Diffusive emanation If the recoil energy is not large enough or the recoil direction is not directed to the grains border, radon isotopes are not released from the solid grain. However, the radon isotopes still have the chance to leave the grain by diffusion through the mineral lattice. But, due to the very slow diffusion of radon in solid material and the relative short half-lives, the portion of diffusive emanation to total emanation is very small (Tanner (1980), Figure 2.2 E).

The ratio of the number of emanated atoms (N_e) to the number of all produced atoms of an isotope (N_p) is called the emanation coefficient E (also: emanation power, escape ratio, escape-to-production ratio, percent emanation, emanation fraction; Tanner, 1980):

$$E = \frac{N_e}{N_p} \quad (2.2)$$

2.2.2 Dependence of the emanation coefficient on parameters specific to the solid material

The emanation coefficient is not constant. It depends on specific parameters of the emanating solid material. The three main parameters are the *effective inner surface of the grains*, the *water content*, and the *distribution of radium in the grains*.

Effective inner surface The recoil range of radon isotopes in minerals is limited. Hence, it is obvious that smaller grains will have higher emanation coefficients compared to grains with larger diameters. Hence, if a porous media consists of small grains and therefore has a large specific surface, more surface area is available and more radon isotopes can escape from the grains. In theory, the specific surface area of spherical grains increases proportional to the inverse of the diameter of the grains, i.e. $E \propto d^{-1}$. Andrews and Wood (1972), however, found in experiments with sand of different grain sizes that the emanation coefficient of ^{222}Rn increases proportional to $d^{-0.5}$. This stronger dependence is related to the fact that grains in natural soils are not just smooth spheres, but resemble more spherically shaped bodies, being

traversed by cracks and small pores (as shown by Rama and Moore, 1984). These “nanopores” within the soil grains further increase the specific surface of soils. Radon isotopes that emanate into the nanopores can diffuse to the inter-granular pore space and therefore the emanation coefficient of the grains is fostered by the presence of nanopores.

Water content The second important factor influencing the radon isotope emanation is the water content of the porous media. In dry porous media, the proportion of indirectly emanated radon isotopes is increased as the recoil length in air often exceeds the width of the pores. As not all implanted radon nuclei diffuse back from the pockets to the pore space, the overall emanation coefficient is small. In water, however, the recoil length is considerably reduced. The occurrence of water in form of water film around the grains therefore slows the recoiled radon isotopes down and reduces their recoil range. Hence, the probability that recoiled radon isotopes stop in the pore is increased (Tanner, 1980). Sun and Furbish (1995) and Adler and Perrier (2009) theoretically showed the rapid increase of the emanation coefficient of radon isotopes as soon as water films are present.

Distribution of radium in the grains Measured radon isotope concentrations in soil gas and groundwater, but especially the ^{222}Rn concentration, can be larger than expected from the radium content of the soil grains, the grain-size distribution, and the soil water content (Tanner, 1980). The reason for this “radon isotope excess” are radium-enriched coatings around the grains. Hence, the radium is concentrated in the outer areas of the grains and therefore more radon isotopes can escape from the grains to the pore space. The formation of radium-enriched coatings is related to the geochemical and geophysical history of the precursors of both radon isotopes.

2.3 Geophysical and geochemical behavior of the radon isotope precursors

Being part of different decay series, ^{220}Rn and ^{222}Rn have a different number of precursors with different half-lives. In addition, not all preceding elements are the same. The precursors of ^{220}Rn and ^{222}Rn therefore behave differently in response to different environmental conditions, e.g. to the oxygen content of groundwater.

The ^{238}U -series, as host of ^{222}Rn , has two uranium isotopes. Under oxic conditions, uranium is soluble, forming aqueous complexes (Porcelli and Swarzenski, 2003). Hence, uranium is leached from the solid grains during weathering. The daughter products of uranium, however, are insoluble and therefore precipitate shortly after their production on the grains surfaces (Krishnaswami et al., 1982). Therefore, under oxic conditions, the leaching of uranium and the following decay leads to re-deposition of uranium daughters on grains. This process forms coatings of ^{226}Ra -enriched grain surfaces, fostering the ^{222}Rn emanation.

In contrast, in the ^{232}Th -series, no uranium exists and thorium is almost insoluble (Langmuir and Herman, 1980), as are its daughter products under oxic conditions. Therefore, ^{232}Th and its daughter isotopes will remain located at almost the same position in the crystal lattice. Hence, ^{220}Rn precursors can only get relocated to the grains surfaces by recoil into the pore water, from where they precipitate to the grain's surfaces shortly after production (Krishnaswami et al., 1982).

Under anoxic conditions uranium is insoluble (Porcelli and Swarzenski, 2003). In contrast, radium, the direct precursor of both radon isotopes, is slightly soluble (Langmuir and Riese, 1985). Also, because of their redox-chemical behavior, iron and manganese are found dissolved in most anoxic waters. When the anoxic water gets into contact with oxygen, the dissolved radium tends to co-precipitate with iron and manganese oxides/hydroxides on the grains surfaces (Gainon et al., 2007). Thus, iron and manganese covered soil grains are host of radium isotopes. Therefore, iron and manganese coatings foster the emanation of ^{220}Rn and ^{222}Rn to soil gas and groundwater (Greeman and Rose, 1996; Gainon et al., 2007).

However, also the different half-lives of the parent radium isotopes have to be considered. ^{226}Ra , the precursor of ^{222}Rn with a half-life of 1600 y can have accumulated over the last several thousand years. In contrast, the longest-lived radium isotope in the ^{232}Th -series is ^{228}Ra with a half-life of 5.7 y. Hence, ^{228}Ra isotopes must have been deposited within the last 2-3 decades to form “active” ^{220}Rn emanating surfaces. Therefore, the ^{220}Rn emanation is more susceptible to changes of the geochemical conditions that affect the solubility of radium than the emanation of ^{222}Rn .

2.4 The different half-lives of the radon isotopes and the potential resulting application of ^{220}Rn as a natural tracer

Besides the differences of the geochemical history of their precursors, ^{220}Rn and ^{222}Rn differ significantly in their half-lives (55.6 s versus 3.82 d). The different half-lives of the respective radon isotopes affect their respective migration ranges in the subsurface. Hence, due to the longer half-life, ^{222}Rn isotopes are transported by diffusion and advection over larger distances before decay. Therefore, measured ^{222}Rn concentrations in subsurface media integrate the subsurface characteristics, i.e. emanation behavior and transport properties, over larger ranges. In practice, it is not unambiguous to identify if changes of the ^{222}Rn concentrations, measured from subsurface fluids such as groundwater and soil gas, are influenced by mixing with fluids of other ages or by changes of the ^{222}Rn source strength (Hoehn and von Gunten, 1989; Bertin and Bourg, 1994).

In contrast, the migration length of ^{220}Rn is much shorter due to its short half-life. Hence, the ^{220}Rn concentrations of a subsurface media reflect only the very local conditions. Therefore, ^{220}Rn is ideally suited to trace small scale processes that do not affect the dynamics of ^{222}Rn . In addition, as ^{220}Rn is quasi immediately (~ 4 min) in secular equilibrium between radioactive production and decay, the ^{220}Rn concentration is only little affected by transport processes.

Figure 2.3 shows the potential application of ^{220}Rn as a tracer to study the dynamics between surface waters and groundwaters.

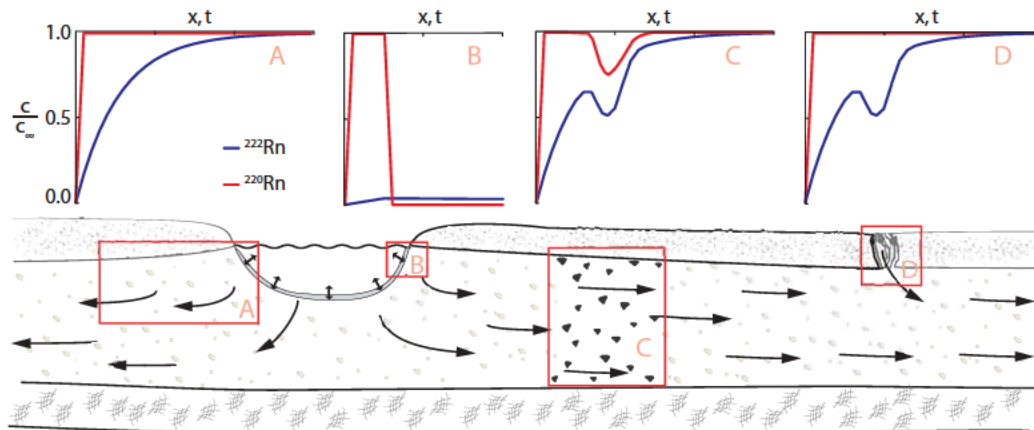


Figure 2.3: Possible applications of ^{220}Rn as a tracer in subsurface fluids, as an example in groundwater. A: undisturbed run of ^{220}Rn and ^{222}Rn concentrations; B: ^{220}Rn as tracer of short term processes; C: identify changing radon isotope source strengths; D: identify the influence of water of other age.

- A: describes the temporal and spatial evolution of the ^{220}Rn and ^{222}Rn concentrations in a undisturbed and homogeneous aquifer. Due to its short half-life, ^{220}Rn reaches its secular equilibrium concentration quasi immediately (approx. 4 min), while ^{222}Rn needs about 16 d.
- B: describes the use of ^{220}Rn as a tracer to study very short term processes, for instance upwelling and downwelling of river water in the river bed. In contrast to ^{222}Rn , ^{220}Rn can be found in the water after a short underground passage because of its short half-life.
- C: describes changes of the emanation of ^{220}Rn and ^{222}Rn in the aquifer material, which can be detected as the concentrations of both radon isotopes are affected.
- D: describes mixing, in this case with younger water. As only the ^{222}Rn concentration is affected by transport processes, the ^{220}Rn concentration remains constant.

2.5 The radon monitor “RAD7”

All radon isotope measurements in this thesis were carried out with the commercially available radon monitor “RAD7” (DurrIDGE Company Inc.). The RAD7 contains a hemispherical measuring chamber of about 0.7 L volume (Figure 2.4). The wall of the chamber is coated with an electrical conductor that lies on positive high voltage (2000-2500 V). By the internal pump of the RAD7, radon containing air is transported into the measuring chamber. To avoid contaminations with solid radon decay products or dust, the air is filtered before the inlet. The detector inside the chamber measures the decay of radon into polonium ($\text{Rn} \rightarrow \text{Po}^+$). The readout system processes the signal and displays the result on a readout screen.

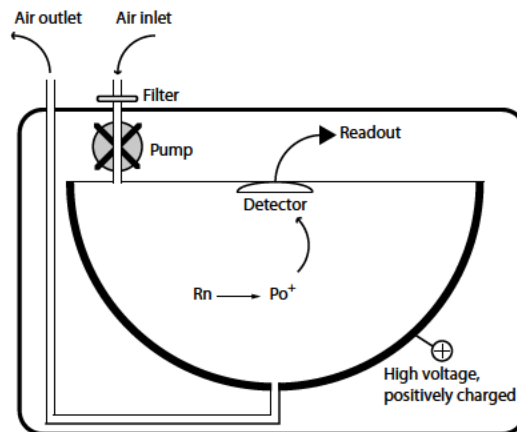


Figure 2.4: Schematic drawing of the RAD7 radon monitor.

Radon, which decays in the measuring chamber, generates positively charged polonium nuclides. By the electrical field in the measuring chamber, the polonium nuclides are directed to and deposited on the planar solid state silicon detector, located at the top-center of the hemisphere. The subsequent decays of the polonium nuclides to lead are registered by the detector. Because of its planar geometry, ~50 % of the polonium decays are registered, hence, if the decay is directed to the detectors surface. By combining the counting rate produced by the decay of polonium, the volume of the measuring chamber, and the pumping rate, the RAD7 yields the actual radon concentration of the introduced air.

The build-in solid-state silicon detector is able to distinguish between different decay energies. Therefore, the RAD7 can distinguish exactly between the different polonium isotopes ^{216}Po and ^{218}Po , and consequently, between the radon isotopes ^{220}Rn and ^{222}Rn , too. The advantage of the simultaneous determination of both radon isotopes makes the RAD7 to the analyzer of choice to determine ^{220}Rn and ^{222}Rn in the environment.

2.6 The natural ^{220}Rn sources used in the laboratory experiments

In laboratory experiments to study the behavior of ^{220}Rn in water and in soil gas under controlled conditions, two different ^{220}Rn sources were used. The used material is purely natural. As it was shown that the annual dose by handling this material will not exceed 1 mSv, both used substances are not subject to any radiological regulation.

For any reliable measurement of ^{220}Rn in water, a ^{220}Rn standard is an utterly needed prerequisite. Unfortunately, up to now, there is no absolute standard available for the ^{220}Rn -in-water analysis. To overcome this limitation and after a rigorous literature search and many experimental tests of different substances, it was finally decided to use natural monazite pebbles as an internal ^{220}Rn -in-water standard to calibrate the ^{220}Rn -in-water analysis protocol.

To simulate the ^{220}Rn production from soil grains and to study the behavior of ^{220}Rn in soil gas in laboratory experiments, a sand was used that had been coated industrially with manganese.

Monazite pebbles

Twelve pebbles of monazite, varying in size between 5 mm and 15 mm, were used as an internal ^{220}Rn -in-water standard. Monazite is a rare-earth phosphate with a typical ^{232}Th content of ~10 % (Anthony et al., 2003). The used pebbles have a



Figure 2.5: Monazite pebbles used as internal ^{220}Rn -in-water standard.

reddish-brown color and are conchoidally to uneven fractured (Figure 2.5). Scanning electron microscope (SEM) pictures of the monazite pebbles indicate a partially weathered mineral surface (Figure 2.6, left). In some areas, the pebble's surface seems to be damaged by the radioactive decay of the isotopes of the ^{232}Th decay series. This damage is indicated by small “holes” (“pleochroitic haloes”) in the mineral surface (Figure 2.6, right).

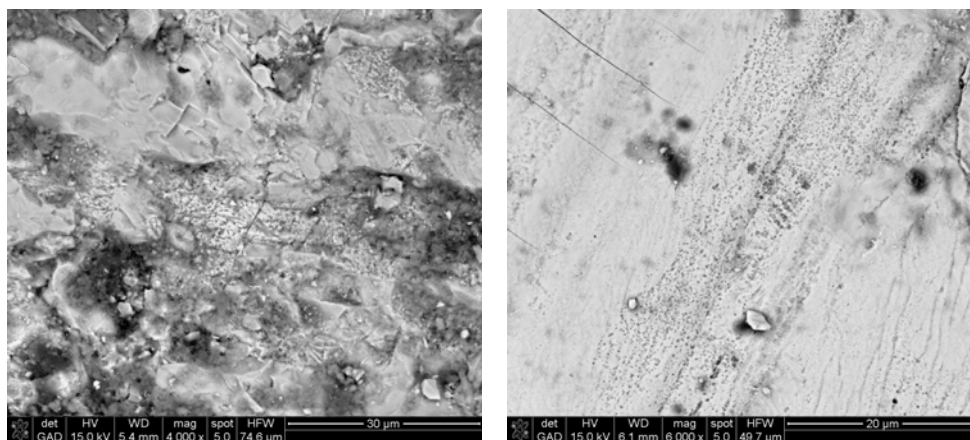


Figure 2.6: SEM pictures of the monazite pebbles. On the left, an example of the partially weathered surface. On the right, “holes” in the surface, suggested to be originated by radioactive decay.

Manganese sand

The manganese sand is a common silicate sand, industrially coated with manganese. The grain size of the sand is mainly between 0.5 mm to 1.0 mm. The

color of the sand is dark-gray to black. The sand was used before as filter material of a bottled mineral water factory to scavenge manganese and radium from the produced mineral water. Therefore, the radium is located with the manganese on the surfaces of the sand grains, producing high amounts of radon isotopes. SEM pictures of the sand (Figure 2.7) show the manganese coatings as an amorphous structure.

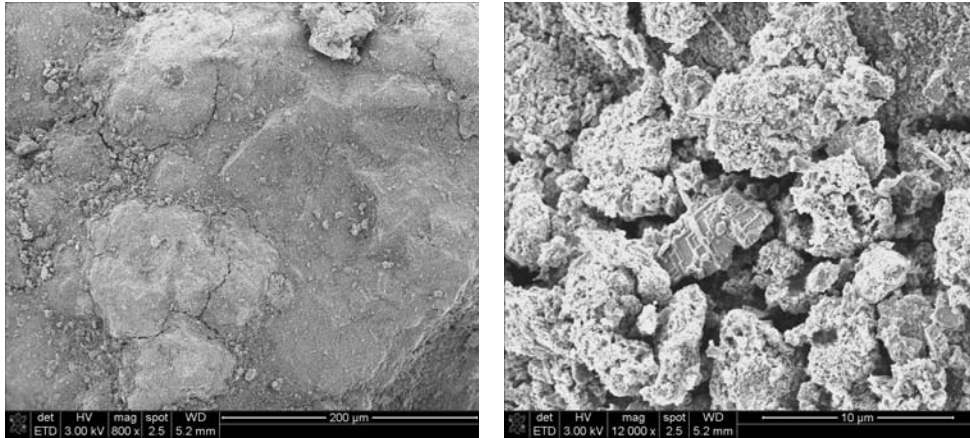


Figure 2.7: SEM pictures of a manganese sand grain. On the left, the manganese coating is shown. On the right, the amorphous structure of the coating is shown in more detail (x 20).

Chapter 3

On the fate of ^{220}Rn in dependence of water content: Implications from field and laboratory experiments

This chapter has been published in collaboration with Matthias S. Brennwald, Eduard Hoehn and Rolf Kipfer in Chemical Geology (Huxol et al., 2012). The supplementary information given in Annex 2 and 3 at the end of this chapter were not included in the Chemical Geology paper.

Abstract To study the potential of ^{220}Rn as a groundwater tracer, we analyzed different groundwater systems with a laboratory-proven radon-in-water detection system. However, with one single exception, no ^{220}Rn was detected in the groundwater, although ^{222}Rn was always present at high concentrations. Field observations of ^{220}Rn and ^{222}Rn in soil gas revealed soil water content to be the crucial control for ^{220}Rn release from soil grains to soil pores. We identified water film around and water menisci between the soil grains to impede the diffusive transport of ^{220}Rn . This finding was confirmed by the results of laboratory experiments with monazite pebbles and manganese sand, which both are ^{220}Rn sources. Besides the water content, the laboratory experiments also identified the water flow (turbulent in the experiment versus laminar in groundwater) to control the ^{220}Rn emanation. The laminar flow condition in groundwater, together with the soil water content, set a conceptual frame to explain why ^{220}Rn can be detected in unsaturated soil but not in groundwater.

3.1 Introduction

The radioactive noble gas radon (Rn) has been used extensively as a tracer in environmental research to study movements of groundwater and soil gas during

the last decades. The most abundant natural radon isotopes are ^{222}Rn with a half-life of 3.82 d, and ^{220}Rn with a half-life of 55.6 s. They are products of the natural decay series of ^{238}U and ^{232}Th , respectively. Radon isotopes are generated by alpha decay from their respective parent radium isotopes ^{226}Ra and ^{224}Ra . As a noble gas, radon is released from radium-bearing mineral grains by recoil and diffusion. Therefore, radon isotopes can be expected to be present in all subsurface fluids i.e. groundwater and soil gas (Andrews and Wood, 1972; Tanner, 1980; Rama and Moore, 1984).

In aquatic systems, the abundance of ^{222}Rn in groundwater is widely used to analyze the groundwater flow, e.g. into oceans (Cable et al., 1996; Burnett and Dulaiova, 2003; Santos et al., 2009), lakes (Kluge et al., 2007; Schmidt et al., 2010; Dimova and Burnett, 2011a), and rivers (Mullinger et al., 2007; Peterson et al., 2010). In aquifers, that are fed by losing rivers, analysis of the ^{222}Rn concentrations along the groundwater flow path allows the determination of bank infiltration rates and the groundwater age (Hoehn and von Gunten, 1989; Bertin and Bourg, 1994; Hoehn and Cirpka, 2006).

In terrestrial systems, the ^{222}Rn abundance in soil gas is extensively applied, e.g. to detect non-aqueous phase liquid-contaminations in soil and groundwater (Hunkeler et al., 1997; Höhener and Surbeck, 2004; Schubert et al., 2007), to analyze and quantify gas transport in soils (Dörr and Münnich, 1990; Lehmann et al., 2000), or to indicate seismic activity (Inan and Seyis, 2010).

The short lived radon isotope ^{220}Rn , however, gained much less interest in environmental research. To analyze ^{220}Rn in water, Burnett et al. (2007) modified a radon-in-water measuring device to detect also the short lived radon species. Using this device, the authors detected ^{220}Rn in water under laboratory conditions and in a single pipe of a public water supply.

In soil gas, the occurrence of ^{220}Rn was used by Lehmann et al. (1999) to assess turbulent air transport near the soil/atmosphere boundary. Giammanco et al. (2007) used ^{220}Rn in combination with ^{222}Rn and CO_2 to determine the origin and to quantify the transport of fumarole gases at Mount Etna.

Our initial motivation to analyze ^{220}Rn in water was to improve the radon groundwater-age dating method by using ^{220}Rn as a co-tracer for ^{222}Rn and the $^{220}\text{Rn}/^{222}\text{Rn}$ ratio instead of the ^{222}Rn concentrations. Because the ^{222}Rn in groundwater concentration along a groundwater flow path is influenced by both, changes in the production of ^{222}Rn and mixing with water of different age, the application of ^{222}Rn as a tool for groundwater dating is rather complex. In contrast to ^{222}Rn , the concentrations of ^{220}Rn in groundwater would be much less affected by mixing due to its short half-life. Therefore, to circumvent the influence of groundwater mixing on the radon-age-dating method, we intended to measure ^{220}Rn in groundwater synchronously with ^{222}Rn and use the $^{220}\text{Rn}/^{222}\text{Rn}$ ratio to date freshly infiltrating groundwaters.

To develop a robust analytical protocol to determine ^{220}Rn in groundwater, we used a modified $^{220,222}\text{Rn}$ -in-water detection system. The system was proven in numerous experiments to determine ^{220}Rn concentrations in water under laboratory conditions (details: see Appendix 3.7). The same system was applied in the environment to analyze the natural ^{220}Rn abundance in 10 different groundwater systems that covered the whole geochemical redox range from oxic to anoxic water (Table 3.1).

Table 3.1: Swiss groundwaters investigated for ^{220}Rn in water. ^{222}Rn was detected in all environments, but not quantitatively measured. +: ^{220}Rn was detected in soil gas.

Aquifer type	Rock type	Water type	^{220}Rn concentration
1 Water adit	Calcium carbonate conglomerate	Oxic spring water	Not detectable (ND)
1 Alluvial fan	Calcareous marlstone	Oxic spring water	ND
1 Gravel-sand	Carbonate-silicate gravel	Oxic groundwater	ND +
2 Gravel-sand	Carbonate-silicate gravel	Sub-oxic groundwater	ND +
1 Gravel-sand	Carbonate-silicate gravel	Anoxic groundwater	ND +
1 Weathered rock	Clay schist	Anoxic groundwater	ND
1 Fractured rock	Travertin marble	Anoxic thermal spring water	ND
1 Fractured rock	Clay schist	Anoxic mineral groundwater	ND
1 Fractured rock	Clay schist	Anoxic mineral spring water	$1.4 \pm 0.13 \text{ Bq/L}$

However, in only one single anoxic spring ^{220}Rn was detected in water. This spring is intensively exploited for bottled water production and is therefore tapped by metal tubes. The interior of the production pipe, from which we sampled the water for radon analysis, is completely coated with iron and manganese precipitates. Such deposits within a pipe are known to accumulate radium by co-precipitation and therefore are a strong source for radon isotopes (Valentine and Stearns, 1994; Fisher et al., 1998). In contrast, no ^{220}Rn was detected in all other examined groundwater systems, although ^{222}Rn was always present at concentrations typical between 10 Bq/L and 30 Bq/L.

To study the reason for the general absence of ^{220}Rn in groundwater despite its ubiquitous presence in soil gas, we redirected our studies towards continuous field-measurement of both radon isotopes in soil gas. Based on these results, we developed a conceptual model describing the release of ^{220}Rn from soil grains to soil gas under changing soil water content. With laboratory experiments we tested and validated the developed conceptual model, which finally allows us to explain the general absence of ^{220}Rn in groundwater.

3.2 Continuous measurements of ^{220}Rn and ^{222}Rn in a natural soil

To determine both radon isotopes concentrations in soil gas in the field, we used the radon analyzer RAD7 (DurrIDGECompany Inc.). Soil gas was sampled using polypropylene membrane tubes (Accurel® PP V8/2). The Accurel® tubes are chemically inert, mechanically stable, hydrophobic and permeable for gas, but not for liquid water up to pressures of 350 kPa (Schubert et al., 2008). To sample radon along a vertical soil profile, we installed 1 m long membrane tubes in horizontal slits of a trench in depths of 0.02 m, 0.10 m, 0.40 m, 0.80 m and 1.20 m. At each depth, in order to complement the radon analysis, we installed sensors to measure soil temperature and soil water content (5TE, Decagon Devices Inc.). After installation, the trench was re-filled with the original soil, attempting to re-establish the original soil layering.

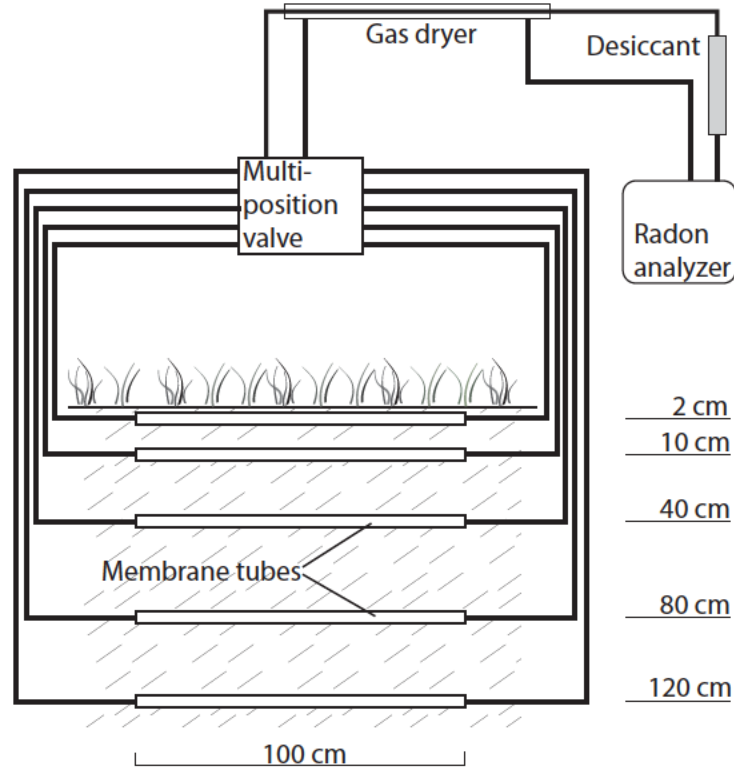


Figure 3.1: Sampling setup for measuring radon isotopes in soil gas.

The sampling tubes were connected as distinct sampling loops to an automatic multiposition valve using PVC tubings. The valve allowed individual membrane tubes from the different soil depths to be connected to the radon analyzer (Fig-

ure 3.1), while the internal pump of the radon analyzer recycled the gas within the selected sampling loop. The automatic valve was operated to sequentially switch from the top sampling tube downward, whereby at each sampling depth the $^{220,222}\text{Rn}$ concentrations were determined for 1 hour. After finishing the depth profile, the radon analyzer was purged for one hour with atmospheric air which can be regarded as virtually free of radon isotopes (Lehmann et al., 2001). Then the measurements started again from the top. As one sampling cycle took 6 hours, each depth was sampled 4 times every day for one hour (hourly mean $^{220,222}\text{Rn}$ concentrations every 6 hours). Soil temperature and soil water content were measured every hour.

The soil gas sampling installation was set at 30 m distance from a losing river and was operated before and during a flood event being caused by strong rainfall and snowmelt. Due to the elevated river runoff, the groundwater level rose by ~ 1 m and submerged the lowermost sampling tube. Simultaneously with the sharp increase of the soil water content in the depth of 1.2 m, the concentrations of both radon isotopes decreased considerably (Figure 3.2). During saturated conditions, the ^{220}Rn concentrations dropped to virtually zero, whereas the ^{222}Rn concentrations decreased by about 40 %. After the flood event, simultaneously with the decrease of the soil water content, the ^{222}Rn concentrations recovered within one day, reaching concentrations similar to those before the event. The ^{220}Rn concentrations, however, only barely recovered. Furthermore, at the end of the experiment, the ^{220}Rn concentrations only reached a maximum of 20 % of the value of the soil conditions before the event, but also the soil water content stabilized on higher level than before the event.

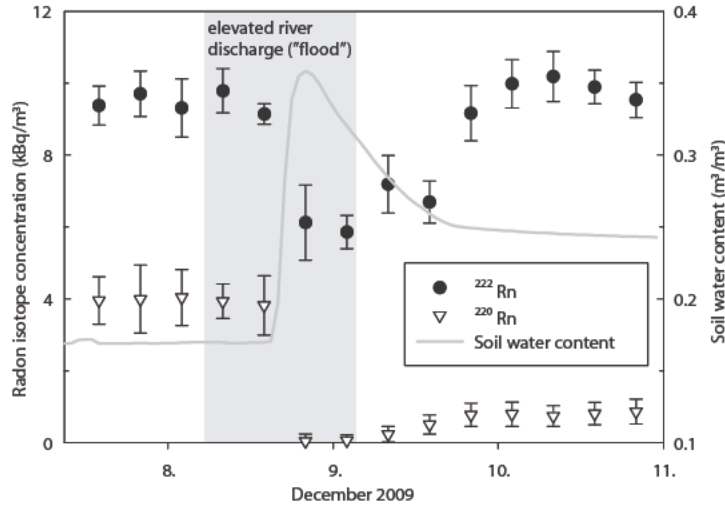


Figure 3.2: Concentrations of ^{222}Rn and ^{220}Rn , and soil water content during flooding of the membrane tube at a depth of 1.2 m.

Although laboratory experiments with the Accurel® tubes might indicate that the diffusion rate of radon through the membrane could be too small to detect ^{220}Rn in water (Surbeck, 1996), the field observations imply that the ^{220}Rn abundance in soil gas is strongly related to the water content of the porous media.

3.3 Conceptual model of ^{220}Rn release from soil grains to soil gas

To explain observed changes of ^{220}Rn concentration and to understand the functional relation to the soil water content, we formulate the following conceptual model. The model is based on the emanation process which accounts for the release of radon isotopes from the mineral grain matrix to the soil pores.

Two mechanisms govern the emanation of radon from solids, namely recoil as a consequence of radioactive decay and production, and diffusive transport in fluid (Rama and Moore, 1984).

The radon isotopes ^{220}Rn and ^{222}Rn are produced by alpha decay of their precursors ^{224}Ra and ^{226}Ra . During decay, ^{220}Rn and ^{222}Rn are recoiled from their position within the crystal lattice. The length of the displacement of the radon nuclides depends on the isotope specific recoil energy and the medium that surrounds the location of radioactive disintegration (Table 3.2). If a grain boundary is located within the recoil range of decaying radium nuclides, radon isotopes can be ejected from the solid material (Tanner, 1980). Hence, some of the radon nuclides are recoiled directly to soil pores of the intergranular pore space. Others escape to small internal pores of the grains (“nanopores”), from where the radon isotopes can migrate by diffusion to the larger soil pores (Rama and Moore, 1984).

Table 3.2: Recoil energies and path lengths of ^{220}Rn and ^{222}Rn due to recoil and diffusive transport in different media. Diffusion lengths are calculated with equation 3.1 and the radon diffusion coefficients in water: $D_{\text{wat}} = 10^{-9}\text{m}^2/\text{s}$ (Andrews and Wood, 1972); and in air: $D_{\text{air}} = 1.2 \cdot 10^{-5}\text{m}^2/\text{s}$ (Hirst and Harrison, 1939). ^(a): Bossus (1984), ^(b): Tanner (1980). (- : no available data)

	Recoil energy (keV)	Recoil range (10^{-6} m)			Diffusion length l_D (10^{-3} m)	
		Minerals	Water	Air	Water	Air
^{220}Rn	103 ^(a)	-	-	83 ^(b)	0.28	31
^{222}Rn	83 ^(a)	0.02 - 0.07 ^(b)	0.1 ^(b)	63 ^(b)	22	2390

Being liberated from the crystal lattice by recoil, and as long as advective soil gas transport is negligible, diffusion is the dominant migration process of the radon isotopes. The diffusion length (l_D) of ^{220}Rn and ^{222}Rn is given by (e.g. Tanner (1964)):

$$l_D = \sqrt{D/\lambda}, \quad (3.1)$$

where D is the diffusion coefficient and λ the decay constant of the respective radon isotope ($\lambda = \frac{\ln(2)}{T_{1/2}}$, $T_{1/2}$: half-life).

l_D define the spatial scale after which the initial concentration of the respective radon nuclides is reduced to $1/e$. It depends on the specific half-life and the diffusion coefficient of the type of media that is being crossed (for typical values see Table 3.2). For macroscopic diffusion throughout porous media like soils, D has to be replaced by the soil-specific effective diffusion coefficient D_{eff} .

As the diffusion coefficient in water is about 10^4 times smaller than that in air, the diffusion length of both radon isotopes in water is more than two magnitudes lower than in air. Due to its shorter half-life, the diffusion length of ^{220}Rn in water and air is 10^2 times smaller than that of ^{222}Rn .

Due to capillary forces, with increasing soil water content, first the nanopores within the soil grains are expected to be filled with water. At these conditions, much of the short-lived ^{220}Rn is not able to reach the intergranular pore space (Rama and Moore, 1984). With increasing soil water content, the water film around the soil grains are also expected to become thicker. Once the water film reach a critical thickness, they effectively stop the recoiled radon nuclides. Under such “wet” conditions, the transfer of the radon gas molecules from the grains into the soil gas is mainly controlled by diffusion within these water layers. During the transfer through these water films a significant fraction of the ^{220}Rn will decay within the water before being released into the soil gas. In contrast, most of the ^{222}Rn will still pass the water film because its diffusion length is larger than the water film thickness due to its much longer half-life. Hence, increasing soil-water content is expected to lead to thicker water films which in turn increase the transfer time of radon isotopes to reach the gas filled pores and consequently reduces the ^{220}Rn concentration in soil gas.

Moreover, even if a fraction of ^{220}Rn reaches the soil gas, the migration of ^{220}Rn throughout the soil is strongly limited by water menisci between the soil grains. Such water menisci separate different gas filled pore-space domains from each other and therefore reduce the effective permeability of soils (Rogers and Nielson, 1991).

Acknowledging all these factors controlling the radon emanation, we hypothesize that the water content of soils strongly controls the release and migration of the short lived ^{220}Rn in the pore space of the soil. ^{222}Rn , however, is much less influenced by the soil water content due to its much longer half-life. Hence, ^{222}Rn and ^{220}Rn are fractionated during their release from the grains and their migration throughout the soil by their significant different diffusion lengths.

3.4 Experimental setup to test the conceptual model

To test our conceptual model of ^{220}Rn emanation, we performed targeted laboratory experiments to analyze the release of ^{220}Rn from different substrates (monazite pebbles and manganese sand) under different wetting conditions. Whereas the monazite pebbles simulate the mineral grain matrix of a soil in a very artificial manner, the manganese sand (Mn-Sand) mimics the situation of ^{220}Rn release from natural porous media reasonably well.

The measurements of the ^{220}Rn release were conducted using the experimental setup shown in Figure 3.3, using a RAD7 radon-in-air analyzer to measure ^{220}Rn and ^{222}Rn concentrations. In a first experiment we used ~ 80 g of monazite pebbles with diameters between ~ 5 mm and 15 mm. These monazite pebbles were also used to test the performance of our radon-in-water detection system (see Appendix 3.7). The rare-earth phosphate mineral monazite has a typical ^{232}Th content of about 10 wt% and is therefore a suitable ^{220}Rn source for experiments. The release of ^{220}Rn from the monazite pebbles was determined under different wetting conditions (dry, wet surface, covered with ~ 1 cm radon-free water). In addition, the response of the ^{220}Rn release to enhanced air turbulence and to sparging the water was analyzed with and without operating an aquarium stone as an air diffuser (Figure 3.3). Every single scenario was maintained for 30 minutes, yielding 6 separate five-minute measuring cycle values with a 1σ counting error.

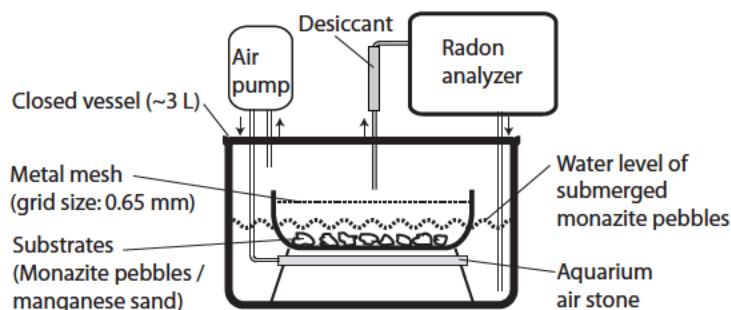


Figure 3.3: Closed vessel (volume 3 L) with radon analyzer for testing the release of ^{220}Rn from different substrates. The substrates were placed in a metal basket. An air diffuser (aquarium air stone) below the basket (fed by the air pump) was optionally used to enhance the circulation of air and water around the monazite pebbles. The metal mesh between the substrates and the radon analyzer inlet was placed to reduce turbulent flow.

In the second experiment, we repeated the first experiment but used 200 g of manganese sand as substrate. The Mn-sand was previously used to scavenge manganese and radium from natural mineral water. The sand grains are therefore coated with radium bearing manganese oxides. Before starting the experiment, the Mn-sand was dried at 105°C for 24 hours to remove all residual water. During the

experiment, a few mL of radon-free water were added stepwise to the sand and homogeneously distributed, until the Mn-sand was completely saturated (water content ≥ 0.4). In each wetting step, the release of ^{220}Rn from the sand was analyzed for 30 minutes, yielding the mean and standard deviation of 6 separate five-minute measuring cycle values.

As the exact volume of the vessel could not be determined we use the specific ^{220}Rn activity cpm (count per minute) as unit to compare the different ^{220}Rn emanation efficiencies. Under the given experimental conditions, the determination of the ^{222}Rn release was not feasible. Due to its longer half-life it takes about 21 days to reach equilibrium between production and decay. Over such a long period it was not possible to adequately control the water content of the substrates.

3.5 Results and discussion

3.5.1 Influence of water content

In the first experiment, the dry monazite pebbles produced a mean ^{220}Rn activity of ~ 105 cpm (set as reference: 100 %, Figure 3.4a). Wetting the surfaces of the monazite pebbles reduced the ^{220}Rn activity by a factor of 20 to ~ 5 %. Such reduction is consistent with our conceptual model, i.e. that a water film around the monazite pebbles reduces the release of ^{220}Rn to the air. By completely submerging the monazite pebbles under water, the ^{220}Rn activity became virtually zero. In this case, the ~ 1 cm layer of water clearly exceeded the diffusion length of ^{220}Rn and hence totally blocked the diffusive transport from the monazite pebbles into the air.

Operating the aquarium stone yielded a similar relationship between the observed ^{220}Rn activity and the wetting conditions. These results will be discussed in detail in Section 3.5.2.

The similar experiment with the Mn-sand also identifies the water content as a controlling factor for ^{220}Rn emanation. The dry Mn-sand showed a ^{220}Rn activity of ~ 12 cpm (Figure 3.5, I). The ^{220}Rn activity considerably increased to ~ 20 cpm when the first few mL of water were added. Additional adding of small amounts of water further increased the ^{220}Rn activity until it reached a maximum (~ 35 cpm) for water contents from 0.07 to 0.25 (Figure 3.5, II). The observed activity increase for small water contents can be understood by the conceptual model of Tanner (1980): water film around the sand grains impedes that ^{220}Rn nuclei are implanted into adjacent sand grains. Hence, the probability that ^{220}Rn nuclei stop within the pore space and can escape from the pore matrix is greatly increased (Tanner, 1980).

At a water content of 0.25 and higher, the ^{220}Rn activity decreased with in-

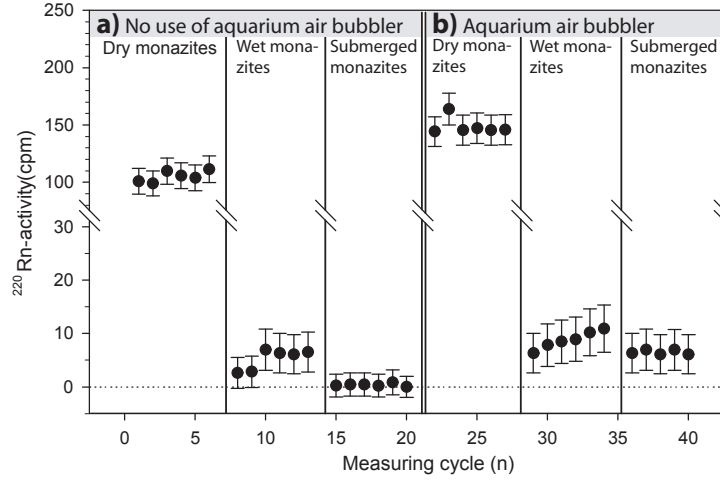


Figure 3.4: Activity of the monazite pebbles at different wetting conditions, without (a) and with induced air flow (b). Note the break on the y-axis, above and below which, different scales were used.

creasing water content (Figure 3.5, III). At a water content ≥ 0.34 , virtually no ^{220}Rn was detected. According to our conceptual model, this decrease corresponds to the suppression of the ^{220}Rn release by a sufficiently thick water film. Sun and Torgersen (1998) report similar findings while studying the release of ^{220}Rn from ^{224}Ra -coated manganese fiber under various wetting conditions. In addition, with increasing water content, water menisci separate individual gas filled pores of the sand and therefore decrease the effective diffusion coefficient of the sand. Hence, towards the end of the experiment, the fraction of sand that still allows ^{220}Rn to be released is reduced.

3.5.2 Influence of turbulence

In the other part of the experiment targeting on the ^{220}Rn emanation of the monazite pebbles, the aquarium stone was operated in order to foster the turbulent mixing in the closed vessel (Figure 3.4b). Forcing air “through” the dry monazite pebbles increased the ^{220}Rn activity by $\sim 40\%$, most probably due to the enhanced advective transport of ^{220}Rn from the monazite pebbles towards the radon analyzer.

However, by applying the air stream on the wet monazite pebbles, we determined a gradual increase of the ^{220}Rn activity from 6 % to 10 %. We assume that the enhanced turbulence in the air around the monazite pebbles produced shear stress on the transport-limiting water film and therefore reduced their thickness.

In response to operating the aquarium stone on the submerged monazite pebbles, the ^{220}Rn activity increased slightly to $\sim 6\%$. Again, we assume that the

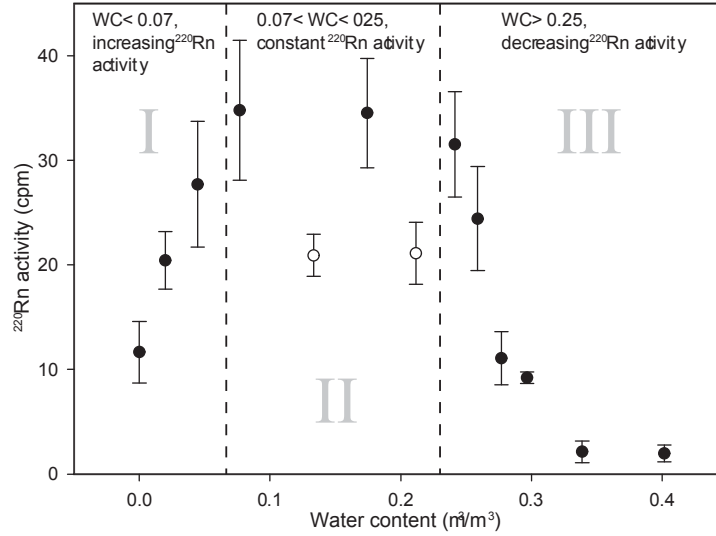


Figure 3.5: Activity of the Mn-sand measured in a closed vessel at different wetting conditions. Empty circles delineate outliers, probably due to incomplete sealing of the measuring vessel.

air bubbles produced turbulence and therefore induced shear stress on the nearby water around the monazite pebbles. This fostered gas/air exchange, i.e. ^{220}Rn nuclei that were set free from monazite pebbles were picked up by air bubbles and transported to the free air of the measuring vessel.

3.5.3 Implications of the results for ^{220}Rn -in-water measurements

Our results, especially with respect to turbulent mixing, give some insights why ^{220}Rn can be detected in water only under some special circumstances. In our laboratory experiments (see Appendix 3.7), in the tapped mineral water spring (see Table 3.1), and in the study of Burnett et al. (2007), always fast flowing water was present. Under this condition, water flow is turbulent and seems to produce sufficient shear stress to disturb and reduce stagnant water film around the ^{220}Rn producing mineral grains. Consequently, turbulence allows ^{220}Rn to reach the mobile water phase, which transports ^{220}Rn to the detection system.

In our laboratory experiment to test our ^{220}Rn -in-water detection system, ^{220}Rn was detected in the water phase surrounding the submerged monazite pebbles. In this experimental setup, the used pump generated a fast and strong water flow around the monazite pebbles. Such turbulent flow enabled ^{220}Rn to emanate from the monazite pebbles into the flowing water and finally to reach the detector.

The occurrence of ^{220}Rn in the anoxic mineral water from a tapped spring seems to be also related to turbulent flow within the pipe (see Introduction). The

water in the production pipe had a velocity of ~ 35 cm/s. The induced shear stress allowed the flow water to gather the ^{220}Rn , being produced from the pipes inner iron and manganese coatings. Under similar conditions, Burnett et al. (2007) were able to detect ^{220}Rn in water from a water supply pipe in New Jersey, USA.

Under such “fast flow” conditions, the ^{220}Rn occurrence in water seems to be functionally controlled by shear stress. This shear stress renders the ^{220}Rn emanation to water and its detection possible.

In contrast, during sampling for radon analysis from groundwater, the typical groundwater flow velocities around the extraction well are very small and do strongly decrease with increasing distance. Due to the small flow velocities and the small pore diameters in porous aquifers, the typical Reynolds numbers are much smaller than the critical Reynolds number for turbulent flow (Freeze and Cherry, 1979). Therefore, in porous aquifers, the groundwater flow is in general laminar and groundwater velocities are much too small to produce any further shear stress on the pore matrix. The pumping induced groundwater flow therefore does not significantly affect the stability of stagnant water layers around the grains of the matrix. Hence, in natural groundwaters, the water flow velocities induced by pumping do not stimulate the ^{220}Rn release, which in turn remains therefore negligibly low.

In addition, due to the significant differences in half-lives and migration lengths of the radon isotopes, the respective sampling volumes from where the radon isotopes are abstracted differ considerably. The sampling volume of ^{220}Rn is 3-4 orders of magnitudes smaller than that of ^{222}Rn . The very constricted sampling volume in combination with the low flow velocities in groundwater conceptually explain why the long-lived ^{222}Rn , but not the short-lived ^{220}Rn , is generally found in groundwater.

3.6 Summary and conclusion

To explore the potential of ^{220}Rn as a novel groundwater tracer, we analyzed the radon isotope concentration in 10 different groundwaters using a tailored radon-in-water detection system (Appendix 3.7). However, 9 of the investigated groundwaters did not contain any detectable ^{220}Rn concentration, even though our detection system was proven to detect ^{220}Rn under laboratory conditions.

In field experiments analyzing the ^{220}Rn concentrations in soil gas under different wetting conditions, soil water content was identified as a crucial control of ^{220}Rn emanation.

Laboratory experiments proved that the ^{220}Rn release from different substrates is mainly a function of water content. Results of laboratory experiments agree with the conceptual model of Tanner (1980) and confirm that low water con-

tent stimulates ^{220}Rn emanation. Our experimental finding that high water content suppresses the ^{220}Rn release is in line with our developed conceptual ^{220}Rn emanation model. This model identifies water film and their thickness to impede the release of ^{220}Rn from solid grains to soil gas. Further, the laboratory experiments under saturated conditions tag shear stress caused by the turbulence at high water flow velocities to significantly enhance the ^{220}Rn release. These two factors - soil water content and flow velocity - functionally determine ^{220}Rn occurrence in granular aquifers. As a consequence, the saturated condition in concert with slow laminar groundwater flow strongly limit the ^{220}Rn occurrence in groundwater to a negligible level in natural aquatic environments.

Our study is a step forward to a better understanding of the emanation process and the fate of radon isotopes in groundwater and soils. In particular, the small diffusion length ^{220}Rn in water is identified as the physical basis why ^{220}Rn does commonly not occur in groundwater. As a result, ^{220}Rn is commonly not applicable as a tracer in groundwater. In unsaturated soils however, the water content is commonly low enough to allow ^{220}Rn to emanate from the soil matrix to soil gas. Therefore, in soil ^{220}Rn is a valuable tracer, e.g. to study soil gas transport in the top-layers of soils.

Acknowledgments

We thank Evelin Vogler for her help measuring soil gas in the field. Heinz Surbeck is thanked for his helpful comments and fruitful discussions. We thank Stefano de Francesco and Natasha Dimova for their thoughtful comments, helping to improve the manuscript. This work was financed by the Swiss National Science Foundation (SNF-projects 200021-119802 and 200020-135513).

3.7 Annex 1: ^{220}Rn -analysis in water: Method

To determine both radon isotopes in water, we used the radon-in-air analyzer RAD7 (DurrIDGE Company Inc.) in combination with the spray chamber RADAqua. The system was optimized to reduce the residence times of water and air in the system by coupling an additional air loop to the radon analyzer (see Figure 3.6 and Dimova et al., 2009). Besides the RADAqua unit, we tested the use of the membrane contactor capsule MiniModule[®] (LiquiCel[®]) as an alternative degassing unit for radon isotope-in-water analysis. The membrane capsule was found to be more efficient to separate radon from water than the spray chamber. However, particulate matter in the sampled water can clog the capsule. Consequently, in

dependence of the turbidity of the analyzed water, we chose the appropriate degassing system, either the RADAqua or the MiniModule.

To our knowledge, there is no absolute standard available for the ^{220}Rn -in-water analysis. As an internal ^{220}Rn standard for our experiments, we used pebbles of the rare-earth phosphate mineral monazite. Monazite is an appropriate ^{220}Rn source as it has a typical ^{232}Th content of $\sim 10\text{ wt}\%$. To test the performance of our ^{220}Rn detection system we used $\sim 80\text{ g}$ of the monazite pebbles with diameters between $\sim 5\text{ mm}$ and 15 mm .

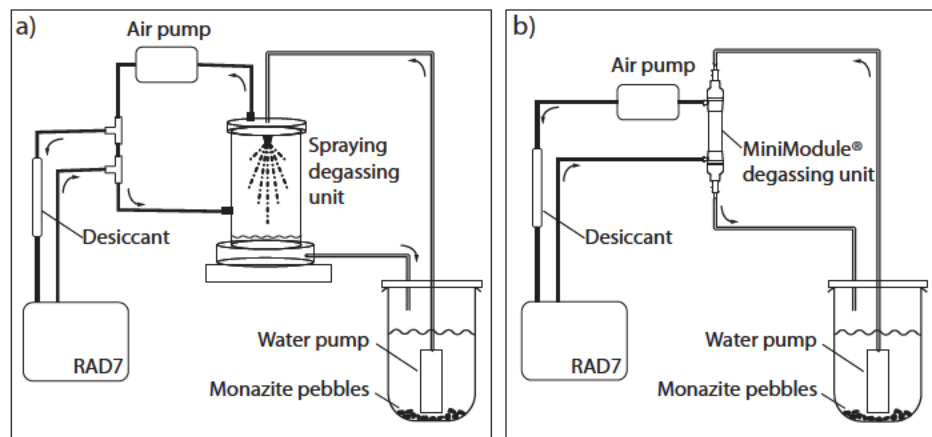


Figure 3.6: Sampling systems for analyzing ^{220}Rn and ^{222}Rn in water. a) setup for increased turbidity, modified after Dimova et al. (2009). b) setup with MiniModule[®] degassing unit, for low turbidity.

Using the monazite pebbles, we calibrated and tested the degassing systems in laboratory experiments (Figure 3.6). After filling the water vessel with 3 l of radon-free water, the performance of the radon analyzing system was determined by applying different water and air flows to optimize the detection system.

The performance for ^{220}Rn -in-water detection of both degassing units (RADAqua and MiniModule) was found to be strongly dependent on the applied water and air flow: the effective ^{220}Rn count rate increases with increasing water and air flows (Figure 3.7). Over all, due to its smaller volume, the MiniModule commonly yielded higher activities in the radon analyzer than the RADAqua for any given water and air flow.

In the field, we used the experimental setup as in the laboratory experiments (see Figure 3.6), except that extracted groundwater was not circulated, but continuously fed through the degassing systems. Both degassing systems were used extensively in field experiments studying different groundwaters that cover the environmental range for swiss groundwaters from oxic to anoxic water. However, most investigated groundwaters were found to be virtually void of any detectable ^{220}Rn activity (see main text).

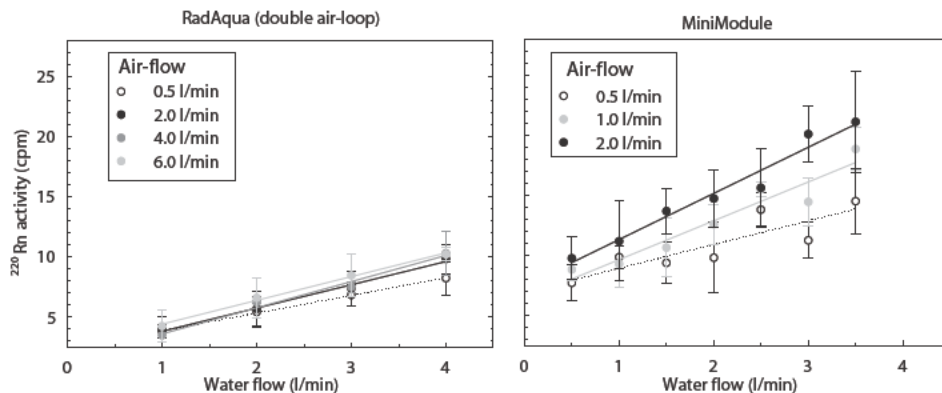


Figure 3.7: Relationship between ^{220}Rn activity and the flow rate of the analyzed water, for various air-flow rates for the coupled RAD7/RADAqua system (left) and for the MiniModule[®] (right), measured using the experimental set-ups of Figure 3.6.

3.8 Annex 2: ^{220}Rn -analysis in water: Results

The only water in which we measured significant ^{220}Rn concentrations was sampled from a mineral water production spring. Sampling was done directly from the production line via a faucet, using the spray chamber as degassing unit (Figure 3.6a). The radon monitor RAD7 was set to measure in five-minute intervals. With the resulting ^{220}Rn -in-air concentration, the ^{220}Rn -in-water concentrations were calculated with the temperature dependent Henry coefficient and corrected for residence time in the sampling system.

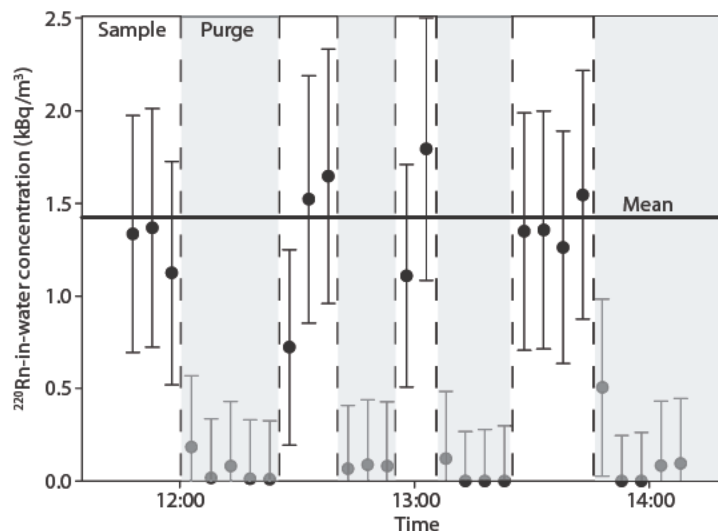


Figure 3.8: ^{220}Rn -in-water concentrations measured from a mineral water well. Alternating sampling and purging method was applied to avoid biases resulting from ^{222}Rn decay products.

However, by testing water with high concentrations of the long-lived ^{222}Rn , the activity of decay products of ^{222}Rn can build up on the detector of the RAD7. This activity biases the ^{220}Rn results determined from the RAD7 device. To avoid such ambiguous results, we fed the RAD7 alternating with air from the spraying chamber and ambient air to purge the measuring chamber with “radon-free” gas.

Figure 3.8 shows the results of the ^{220}Rn -in-water analysis. As the no significant ^{220}Rn concentration was determined while testing ambient air, it is assured that the measured ^{220}Rn counts are not caused by the activity of ^{222}Rn decay products, but from the actual decay of ^{220}Rn . In average, the ^{220}Rn -in-water concentration was determined to be $1.4 \pm 0.2 \text{ kBq/m}^3$.

3.9 Annex 3: Emanation of ^{220}Rn from iron and manganese precipitates

As described in Section 2.3, radium isotopes tend to co-precipitate with iron and manganese oxides/hydroxides. Surfaces covered with such precipitates are therefore often spots of strong radon isotope emanation (Gainon et al., 2007).

To analyze the emanation characteristics of ^{220}Rn from such precipitates, we sampled and analyzed the precipitates of two anoxic springs from Switzerland. The water of the Saillon spring is a thermal water. The Rothenbrunnen spring has a cold mineral water that is used for mineral water production. From the latter spring, we sampled precipitates from two sites, from an overflow well and from the mineral water production line.

The precipitates were analyzed by alpha-spectrometry under atmospheric conditions with a 400 mm^2 silicon detector (SARAD Inc.). The determined activities were compared to a thorium standard powder, which is known to have homogeneous radionuclides distribution throughout the material.

Results of the alpha-spectrometric analysis are shown in Figure 3.9. The energy distribution determined from the reference material (plot on top) shows a distinct tailing at energies lower than the decay energy of ^{220}Rn . This indicates that emitted particles had to cross solid material, during which the particles were decelerated and therefore lost energy. The energy distributions determined from the precipitates, in contrast, show much less distinct tailings at lower energies. Hence, the particles emitted from the precipitated material had to cross less solid material. The results confirm that due to its exposed position on the grains and due to its amorphous structure, iron and manganese precipitates with co-precipitated radium act as a strong ^{220}Rn source.

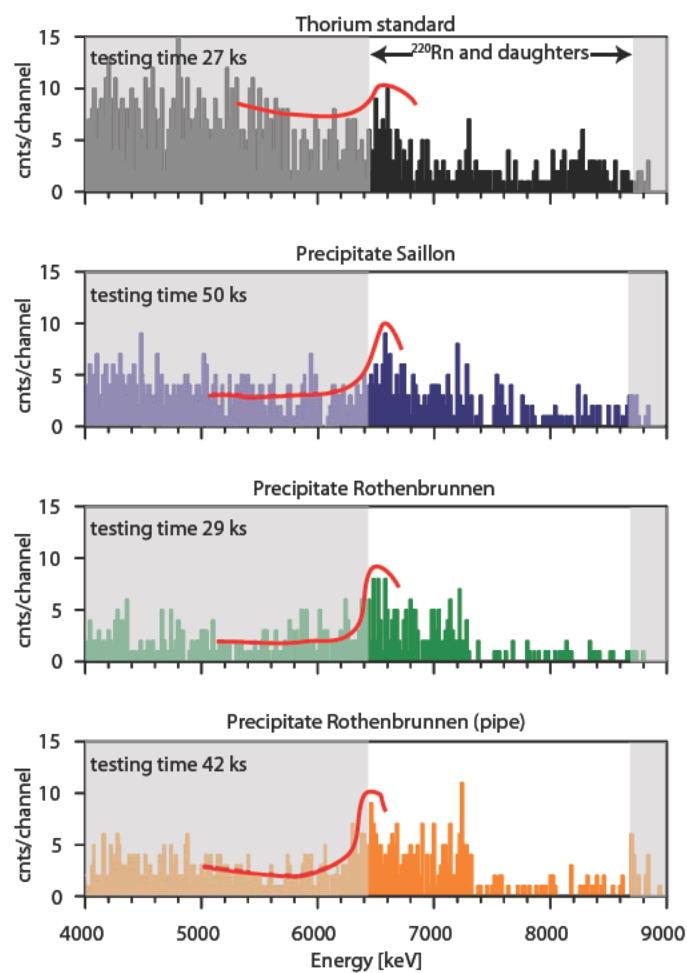


Figure 3.9: Alpha-spectrometric analysis of iron and manganese precipitates compared to powder of a thorium standard. Unshaded area: energy range of ^{220}Rn and its decay products. The red lines are guides to the eye and delineate tailing at lower energies.

Chapter 4

Processes controlling ^{220}Rn concentrations in the gas and water phases of porous media

This chapter has been published in collaboration with Matthias S. Brennwald, and Rolf Kipfer in Chemical Geology Huxol et al. (2013). The supplementary information given in the Appendix at the end of this chapter were not included in the Chemical Geology paper.

Abstract To study why ^{220}Rn is commonly ubiquitous in soil gas but, in contrast to ^{222}Rn , not detectable in groundwater, we conducted targeted laboratory experiments. In these experiments, we used a special, ^{220}Rn productive sand and analyzed the behavior ^{220}Rn in the gas and water phase of the sand under unsaturated and saturated conditions. To simulate changing water contents of soils under unsaturated conditions, we slowly flooded and drained a box filled with the sand and analyzed the resulting dynamics of ^{220}Rn in the gas phase. Under saturated conditions, we analyzed the dependence of ^{220}Rn concentrations in the water phase on water flow by extracting water at different pumping rates from the saturated sandbox and a flow tank filled with the same saturated sand. The results revealed that under unsaturated conditions the migration of ^{220}Rn through the pore space is limited by water menisci between the grains, acting as barriers for ^{220}Rn . Under saturated conditions, the observed dependency of ^{220}Rn concentrations in water on the induced water flow velocity implies that fast flowing water in porous media is able to disturb commonly immobile water layers around the grains and, therefore, stimulate the emanation of ^{220}Rn to the flowing water phase. Extrapolating the finding to common natural conditions, the results explain why ^{220}Rn can be detected in unsaturated soil but not in groundwater. In addition, general conclusions to small scale dynamics of soil gas and groundwater are drawn from the dynamics of ^{220}Rn in subsurface fluids

4.1 Introduction

In the last decades, the naturally occurring radioactive noble gas radon has been used extensively in environmental sciences to trace transport processes in soil gas and groundwater. Radon has two reasonably long-lived isotopes, the most abundant ^{222}Rn (half-life 3.82 d), and the less abundant short-lived being ^{220}Rn (half-life 55.6 s). Both radon isotopes are generated by alpha decay from their radium parents (^{226}Ra and ^{224}Ra , respectively). From radium-bearing solids, the radon isotopes are released by recoil and diffusion (emanation) to the surrounding pore space (Tanner, 1980). Therefore, both radon isotopes are expected to be present in all soil-related fluids such as soil gas and groundwater (Andrews and Wood, 1972; Rama and Moore, 1984; Nazaroff, 1992).

In soil gas, ^{222}Rn is used widely, e.g., to analyze and to quantify soil gas transport (Dörr and Münnich, 1990; Lehmann et al., 2000) and to detect non-aqueous phase liquid-contaminations in soils (Schubert et al., 2001; Höhener and Surbeck, 2004).

In groundwater, ^{222}Rn is used, e.g., to identify and quantify groundwater inflow into surface waters bodies such as oceans (Cable et al., 1996; Dimova et al., 2011), lakes (Kluge et al., 2007; Dimova and Burnett, 2011b), and rivers (Mullinger et al., 2007; Cartwright et al., 2011). Anomalies of the ^{222}Rn concentration in groundwater and springs has been observed in relation to seismic events (Igarashi et al., 1995; Quattrocchi et al., 2000). In groundwaters being recharged by rivers, the residence time of the newly infiltrate water can be determined by analyzing the ^{222}Rn concentrations (Hoehn and von Gunten, 1989; Hoehn and Cirpka, 2006).

In contrast to ^{222}Rn , the shorter-lived ^{220}Rn has received much less attention in environmental sciences. The occurrence of ^{220}Rn in soil gas was used by Lehmann et al. (1999) to assess turbulent air transport near the soil/air interface. In combination with ^{222}Rn and CO_2 , Giammanco et al. (2007) determined ^{220}Rn in fumarole and soil gases to analyze gas transport processes at Mount Etna. Burnett et al. (2007) modified a device for measuring ^{222}Rn in water to determine ^{220}Rn in water. Using this device, the authors detected ^{220}Rn in water in the laboratory, and in the fast flowing water of a supply pipe with radium-containing precipitates at the inner surface.

Due to the very different half-lives of ^{222}Rn and ^{220}Rn (3.82 d versus 55.6 s), the distances that can be passed by the respective radon isotopes before decay (“migration range”) differ significantly. For example, being inversely proportional to the decay constant, the diffusive length scale of ^{222}Rn is about two orders of magnitude longer than that of ^{220}Rn . Therefore, ^{222}Rn concentrations measured in soil gas and groundwater integrate the subsurface transport characteristics over distances of decimeters to meters, whereas ^{220}Rn concentrations reflect only the

very local conditions on the millimeter to centimeter scale. The small migration range makes ^{220}Rn a powerful tool for tracing small scale processes. We therefore proposed to use ^{220}Rn as a natural tracer for small scale processes in aquatic systems, e.g. groundwater (Huxol et al., 2012).

However, despite the general ubiquity of ^{220}Rn in soil gas (Tanner, 1980), we found that under natural water-saturated conditions ^{220}Rn is generally not detectable (Huxol et al., 2012). ^{220}Rn could only be detected in the fast and turbulent flowing water of pipes with radium-bearing precipitates of iron-manganese (Burnett et al., 2007; Huxol et al., 2012). Even under only partially saturated conditions, the water content was found to influence the ^{220}Rn concentrations (Huxol et al., 2012). We hypothesized that immobile water phases in the form of water film around the soil grains together with water menisci between the soil grains delimit the ^{220}Rn migration from the source grains and throughout the pore space. Hence, due to its short half-life, these immobile water phases act as barriers that cannot be passed diffusively by ^{220}Rn , as it decays before it reaches the sampled pore space (Huxol et al., 2012).

To assess the influence of water content on the ^{220}Rn emanation and to evaluate the use of ^{220}Rn as a small scale tracer in soil gas and groundwater, we conducted laboratory experiments in a sandbox (simulating a natural soil column under changing water content conditions) and a flow tank (simulating the saturated conditions of groundwater).

4.2 Material and methods

The experiments were conducted in a sandbox and in a cylindric tank, both filled with the same sand. To analyze the ^{220}Rn concentrations in gas and water, in situ instrumentation is required due to its short half-life. We used a radon-in-air analyzer (RAD7, DurrIDGE Company Inc.), which has an internal air pump that transports the sample gas into the detection chamber. The Rad7 measures and discriminates ^{220}Rn and ^{222}Rn simultaneously by the different decay energies of their respective daughters ^{216}Po and ^{218}Po . For ^{220}Rn in the gas phase, a specific factory calibration is available and has been used. For ^{220}Rn -in-water analysis, the radon analyzer was attached to a modulated degassing system (RADAqua spray chamber with temperature sensor, modified with additional air loop and more efficient nozzle and tubing, described in detail in Huxol et al. (2012)). The ^{220}Rn -in-water concentration was determined from the ^{220}Rn -in-air concentration in the spray chamber by measuring the water temperature and using the temperature dependent partitioning factor of ^{220}Rn between water and air (i.e. the Ostwald coefficient $L = V_{\text{wat}}^{220\text{Rn}} / V_{\text{air}}^{220\text{Rn}}$, Clever and Battino (1979)). The detection limit of the used system for ^{220}Rn -in-water analysis is $\sim 1 \text{ Bq/L}$ (Lane-Smith, 2009).

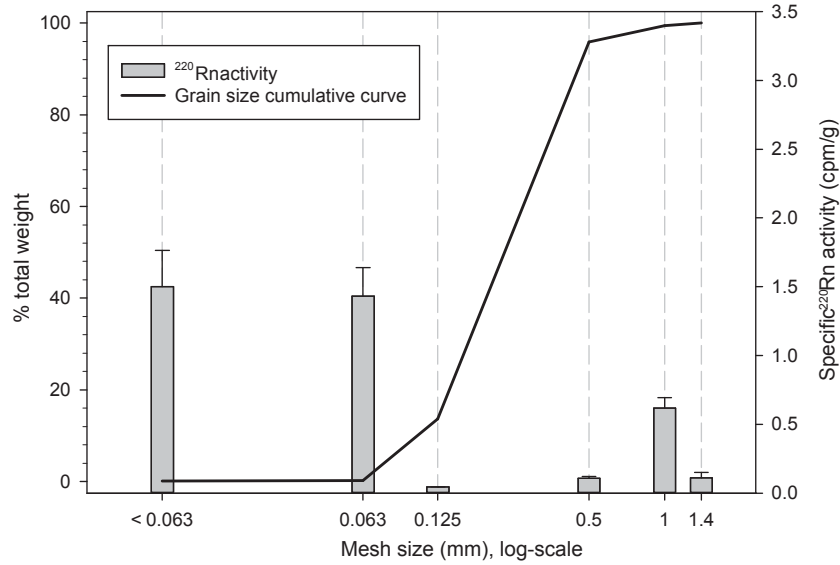


Figure 4.1: Grain size distribution and specific ^{220}Rn activity per grain size of the used sand.

4.2.1 Sand

The sand used for filling the sandbox and the tank is a mixture of two materials: one compound is a sand, which had been coated industrially with manganese. The manganese sand was previously used in a technical application to scavenge radium from mineral water. Due to its radium-rich coating, the ^{220}Rn production of the sand is exceptionally high and hence produced memory effects in the radon analyzer, due to the decay of ^{220}Rn daughter isotopes. We therefore diluted the manganese sand with a common, less radioactive silicate sand in a 1:4 ratio and mixed them in a batch mixer. The resulting sand mixture produces no memory effects, but still allows to measure ^{220}Rn under conditions in which ^{220}Rn would normally not be detectable due to the low environmental abundance of ^{220}Rn .

The porosity of the sand mixture was determined by measuring the mass increase of dry sand due to water saturation. It was found to be ~ 0.45 . The grain size distribution of the sand was determined by sieving. About 82 % of the grains have sizes between 0.5 mm and 1.0 mm, whereby the smallest grains have the largest grain size specific ^{220}Rn activity (Figure 4.1). The higher ^{220}Rn activity is caused by the higher volume-specific surface area of small grains, allowing more ^{220}Rn to escape from the grains (Andrews and Wood, 1972; Rama and Moore, 1984). The total weight-specific ^{228}Ra -activity (air dry) of the sand is $281 \pm 19 \text{ Bq/kg}$, determined by gamma-ray analysis using a germanium well detector.

4.2.2 Sandbox

The sandbox (length: 119 cm, width: 95 cm, and depth: 16 cm; Figure 4.2) was filled up to 75 cm height with water-saturated sand to attain a homogeneous structure of the porous media. After filling, we allowed the sand to dry to a water content of ~ 0.1 .

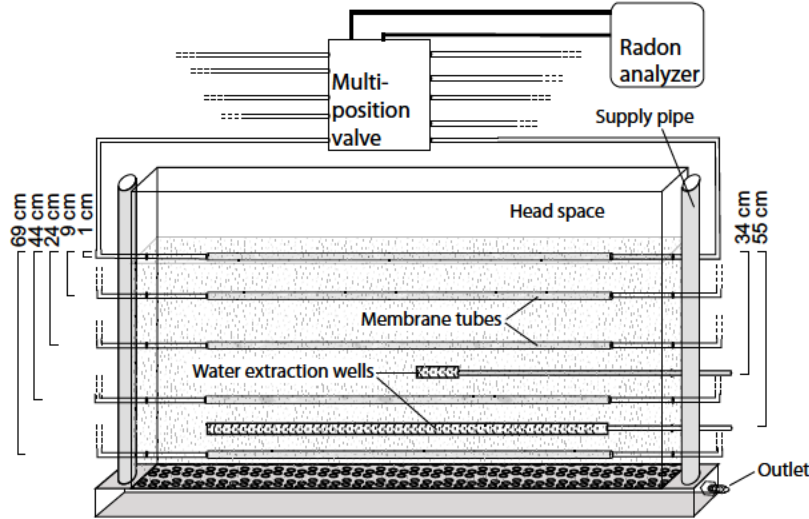


Figure 4.2: Experimental sandbox to study ^{220}Rn in the gas phase of porous media under changing water contents and in the water phase of the fully saturated sandbox. The sandbox was flooded through the supply wells and drained through the outlet. Membrane tubes to sample ^{220}Rn in the gas phase were connected via multiposition valve to radon analyzer (dashed lines at tube endings indicate connection between sandbox and valve, explicitly drawn for uppermost sampling depth). To extract water for ^{220}Rn -in-water analysis, extraction wells (screen lengths 0.1 and 1.0 m) were connected via peristaltic pump to ^{220}Rn -in-water detection system (not shown).

To sample ^{220}Rn from the gas phase of the sand, we installed polypropylene membrane tubes (Accurel® PP V8/2) at different depths of the sandbox. Accurel membrane tubes are chemically inert, mechanically stable, hydrophobic and permeable for gases, but not for liquid water up to pressures of 350 kPa (Schubert et al., 2008). The membrane tubes were coupled over PVC tubes to an automatic multiposition valve, which was used to connect the individual membrane tubes to the radon analyzer (Figure 4.2). The internal air pump of the radon analyzer was used to circulate the gas between the radon analyzer and a particular membrane tube.

At each sampling depth, we additionally installed sensors to measure the water content of the sand (5TE, Decagon Devices Inc.). On both sides of the sandbox, supply pipes were installed to observe and control the water level. Laboratory experiments indicated that the diffusion rate of radon through the membrane is

too small to detect ^{220}Rn in water (Surbeck, 1996). Therefore, to sample ^{220}Rn in the water phase under different flow conditions from the sandbox, two horizontal extraction wells (diameter: 1") of different screen lengths were installed at the depths of 34 cm (screen length: 10 cm) and 55 cm (screen length: 100 cm), respectively. Both extraction wells were connected to a peristaltic pump, which pushed the water to the ^{220}Rn -in-water detection system, consisting of a spray chamber (RADAqua) and the radon monitor (Huxol et al., 2012).

4.2.3 Tank

For water flow experiments, we filled a cylindrically shaped tank (radius: 34 cm, height: 100 cm; Figure 4.3) to a height of 82 cm with the pre-mixed sand. In the center of the tank, a well (diameter: 2") with a screen-length of 10 cm was installed to extract water from the depth of 47 cm. The supply pipe, mounted at the side of the tank and connected to a bottom inlet, was used to fill the tank with water and to recycle extracted water.

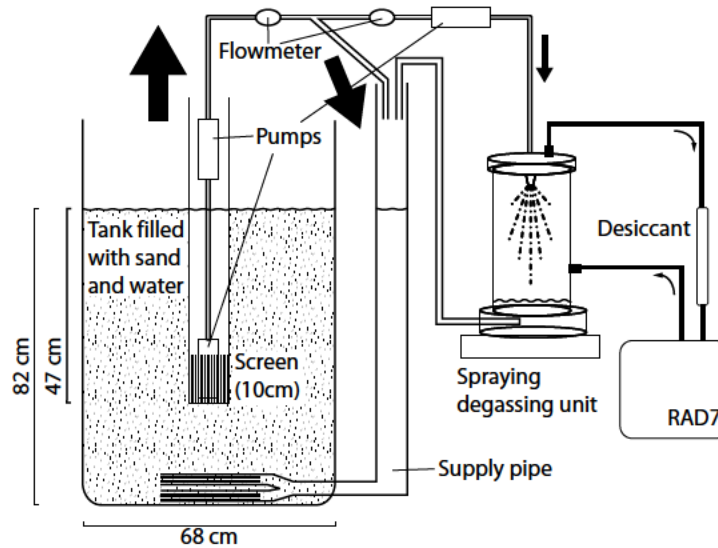


Figure 4.3: Tank filled with sand and water, and installation to withdraw water at different pumping rates. Water discharge through spraying chamber was held constant at 3 L/min, excess water was led to supply pipe (arrows indicate flow direction and flow rate qualitatively). Tank and radon detection device not true to scale.

Water was extracted by a submersible pump (submersible electric pump in combination with an inline electric booster pump, Whale®) at different pumping rates (3-11 L/min). The extracted water passed another separately controlled inline pump to stabilize the flow into the spray chamber of the ^{220}Rn -in-water detection system at 3 L/min (Figure 4.3). Water pumped in excess was led to the

supply pipe.

4.2.4 Experimental work

We analyzed the dynamics of the ^{220}Rn concentration in the gas phase under changing water contents and in the water phase for different flow conditions.

^{220}Rn measurements in the gas phase

We flooded the sandbox from bottom to top through the supply pipes with radon-free water and drained it through the outlet. Simultaneously, we monitored the ^{220}Rn concentrations in the gas phase. During the whole experiment, the water level in the sandbox and the water content of the sand in the different sampling depths were determined every minute. While flooding at a rate of ~ 3 mm/min, the ^{220}Rn concentration in the gas phase was monitored with a time resolution of 2 min, first at the depth of 44 cm. When the water level reached that depth, we continued flooding the sandbox, but now measured the ^{220}Rn concentration in 9 cm depth to repeat the experiment.

While draining the saturated sandbox at a rate of ~ 1 -2 mm/min, we first monitored the ^{220}Rn concentration with a time resolution of 2 min at the depth of 9 cm. When the decreasing water level reached the depth of 44 cm, we measured the ^{220}Rn concentration with a time resolution of 5 min, switching every hour between the two depths. When the water content tended to stabilize at 44 cm depth, we additionally purged the radon analyzer every second hour with radon-free air to prevent memory effects on the radon analyzer. This protocol was continued for 3 days, yielding 8 hourly mean ^{220}Rn concentration values at each depth per day.

^{220}Rn measurements the water phase

From the fully flooded sandbox, we first extracted water from the lower, long extraction well and then from the upper, short extraction well. In both cases the extraction rate was 2.8 L/min. For each well, the ^{220}Rn -in-water concentration was determined with a time resolution of 5 min for a duration of 90 min, yielding the mean ^{220}Rn concentration. After passing the spray chamber for degassing and ^{220}Rn determination, the water was recycled to the sandbox via the supply pipes.

From the tank, we extracted water at different extraction rates (3, 5, 7, 9, and 11 L/min). When switching to a new pumping rate, we allowed the system to flush and to adapt for five minutes. At each pumping rate, we determined the ^{220}Rn concentration for 25 min with a time resolution of 5 min, yielding the mean ^{220}Rn concentration. All water concentrations were corrected for radioactive decay during their respective travel times in tubings from extraction well to detection

system. Uncertainties of all determined ^{220}Rn concentrations are given to the $1-\sigma$ level.

4.3 Results and discussion

4.3.1 Hysteresis of ^{220}Rn in the gas phase

At both sampled depths (9 and 44 cm), the ^{220}Rn concentration in the gas phase showed identical behavior in response to the changing water contents. While floodin the sandbox, the ^{220}Rn concentration in the gas phase decreased considerably, reaching virtually zero when the sand became almost fully saturated (Figure 4.4, “flooding”) These results support the finding of Huxol et al. (2012), who identify the water content of soils as the major factor affecting the ^{220}Rn occurrence in soil gas. In response to increasing water content, water film around and water menisci between the grains develop and grow thicker. Due to its small diffusion coefficient in water and the short half-life of ^{220}Rn , these water phases limit the release of ^{220}Rn from the grains to the gas phase.

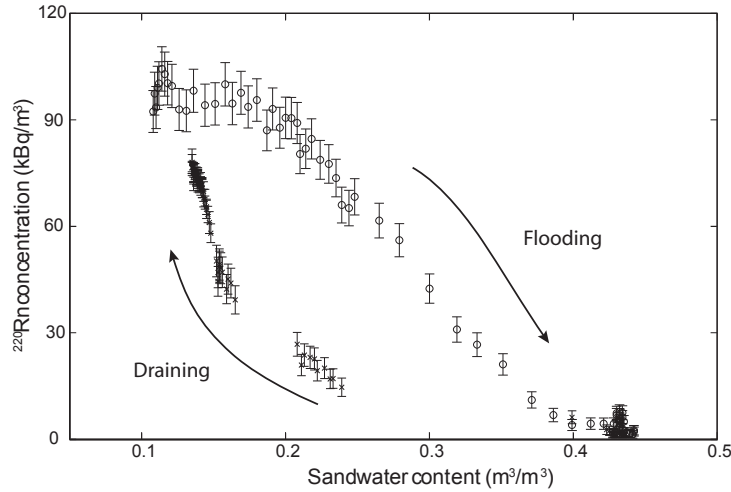


Figure 4.4: ^{220}Rn concentrations in the gas phase during floodin and subsequent draining of the sandbox, shown for the sampling depth of 44 cm. ^{220}Rn concentrations under floodin conditions are consistently higher than under draining conditions, which leads to the observed hysteretic dependence of the ^{220}Rn concentration to soil water content.

While draining the sandbox and thereby reducing the water content of the sand, the ^{220}Rn concentration in the gas phase recovered only partially. Hence, for the same water contents, the ^{220}Rn concentrations determined during the draining situation remained consistently below the ^{220}Rn concentrations measured during the floodin situation (Figure 4.4, “draining”).

The hysteresis behavior of the ^{220}Rn concentration in response to flooding and draining the sand strongly indicates that water menisci are the dominating factor limiting the ^{220}Rn concentration. In natural porous media, the pore space commonly consists of relatively large cavities with narrow connections in between (Jury and Horton, 2004). During wetting the sand, induced by capillary forces, first the narrow connections and small pores are filled with water, later the larger pores are filled too (Jury and Horton, 2004). When the sand gets drained, the pores with larger connections generally start to drain first. However, a fraction of the water can be trapped in larger pores until the narrow connection starts to drain. In addition, after draining, the narrow connections between the pores will retain water in the form of water menisci (Jury and Horton, 2004).

The different distribution of water and the different evolution of the water menisci in response to flooding and draining of the sand could explain the observed hysteresis of the ^{220}Rn concentration. Water-filled pores and water menisci act as barriers for ^{220}Rn as, due to their short half-life, ^{220}Rn decays during their passage through the water phase. Hence, water reduces the permeability of the pore space for gases, and consequently, reduces the migration range of ^{220}Rn and therefore the ^{220}Rn concentration in the gas phase.

4.3.2 Dependence of ^{220}Rn emanation on flow velocity

During the extracting of water from the saturated sandbox, the ^{220}Rn -in-water concentrations were 4.6 ± 0.5 Bq/L at the long extraction well, and 5.8 ± 0.3 Bq/L at the short extraction well (an increase of $\sim 26\%$), both at an extraction rate of ~ 2.8 L/min. As the flow velocity in the sediments in direction to the extraction well is inversely proportional to the surface area of the respective screen, the 10 times smaller screen area of the short extraction well results in 10 times higher flow velocities in the vicinity of the well. Hence, the 10 times higher flow velocity forced the ^{220}Rn -in-water concentrations to increase by $\sim 26\%$.

By using the tank we carried out targeted experiments in order to investigate this effect of (ground-)water flow-velocity on ^{220}Rn -in-water concentrations. Increasing the extraction rate in steps of 2 L/min resulted in corresponding and well-defined increases of the ^{220}Rn concentrations, ranging from 9.1 ± 0.3 Bq/L at a rate of 3 L/min to 9.9 ± 0.3 Bq/L at 11 L/min (an increase of $\sim 9\%$, Figure 4.5). As the extraction rate is proportional to the flow velocity in direction to the well, the flow velocity at 11 L/min is about 3.5 times faster than at 3 L/min. Hence, increasing the extraction rate and therefore the flow velocity by a factor of 3.5 produced $\sim 9\%$ higher ^{220}Rn -in-water concentrations.

Due to the different geometries, the flow conditions in the sandbox and the tank were different (e.g. the sandbox walls bound the radial migration ranges around the extraction wells). Therefore, the absolute ^{220}Rn concentrations from the ex-

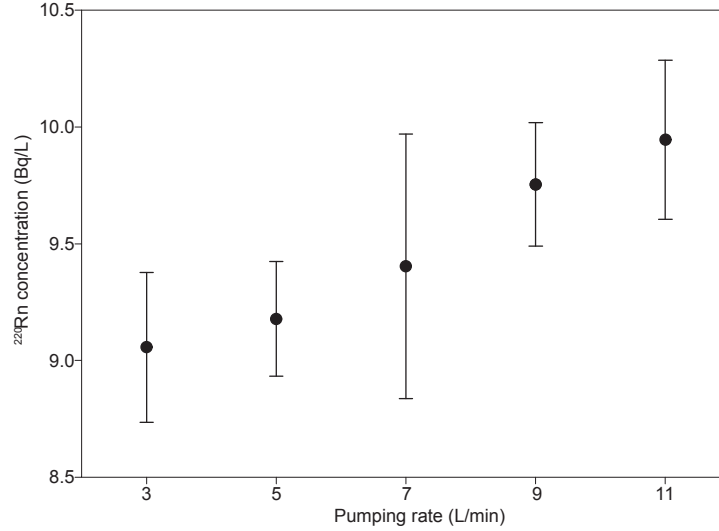


Figure 4.5: ²²⁰Rn-in-water concentrations derived from the sand and water filled tank by applying different extraction rates. Values corrected for radioactive decay during flow through tubing.

periments with the sandbox and the tank cannot be compared directly. However, the relative changes of the ²²⁰Rn-in-water concentrations observed in both systems due to higher flow velocity can be compared. By extrapolation the results of the tank (plus of 9 % at 3.5 times higher flow velocity) to a 10 times higher flow velocity, the ²²⁰Rn-in-water concentrations are expected to increase by ~26 %. This is in good agreement with the observed increase at a 10 times higher flow velocity in the sandbox.

Higher ²²⁰Rn concentrations due to higher groundwater flow velocities are in line with the conceptual view of Huxol et al. (2012). In a natural aquifer with low groundwater flow-velocities, ²²⁰Rn becomes trapped and decays in immobile water layers around soil grains. The high flow velocities in the tank are expected to generate shear stress, which reduces the thickness of the immobile water layers. This increases the emanation of ²²⁰Rn from the grains into the flowing water. Figure 4.6 shows profile of radial flow velocity v from the center of the extraction well to the edge of the tank, calculated for the different extraction rates Q and assessing strictly 2-D flow towards the extraction well ($v(r) = Q/2\pi r h n$, where r is the well radius, h the height of the screen, and n the porosity of the sand). The flow velocity increases proportional to the extraction rate and decreases rapidly with increasing distance to the extraction well. In the area near the extraction well, the flow velocity is high and enforces shear stress. Hence, near the extraction well, the stimulation of the emanation of ²²⁰Rn in response to disturbances of immobile water layers is very plausible.

In addition, at higher extraction rates and hence higher flow velocities, the

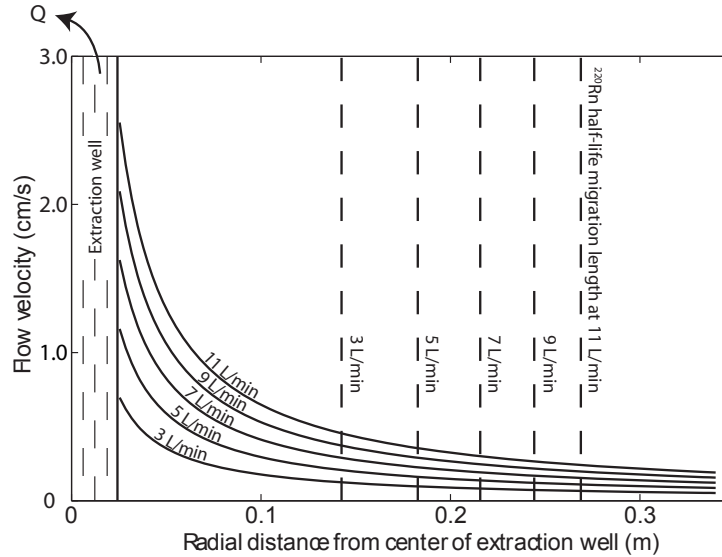


Figure 4.6: Illustrative presentation of velocity profiles induced from different pumping rates Q applied on the extraction well of the tank and assuming strictly 2-D fl w. Vertical dashed lines indicate the respective range from where water is transported within one half-life of ^{220}Rn (55.6 sec).

zone of higher fl w velocities is enlarged and ^{220}Rn is transported over larger distance before decay (vertical dashed lines in Figure 4.6, illustrating the distance traveled in one half-life). Hence, a larger volume and therefore also more ^{220}Rn is sampled.

Our experimental set-up with the high extraction rates and reduced screen area of the extraction well in the tank was intentionally chosen to generate strong shear stress on the immobile water layers by increasing the fl w velocities around the well. Under common natural fiel conditions with far less ^{220}Rn -productive aquifer material, larger screen-surfaces of the extraction wells, and smaller pumping rates, the groundwater extraction for ^{220}Rn analysis in the fiel induces much smaller fl w-velocities. These commonly applied fl w velocities are by far not sufficiently large enough to stimulate the emanation of ^{220}Rn from the aquifer grains to the sampled groundwater and to yield detectable ^{220}Rn concentrations.

The behavior of the inhibited ^{220}Rn emanation under common sampling conditions can be fully understood by extrapolating the results of the laboratory tank experiment to a natural, but still ideal fiel scenario. By assuming a common aquifer material with 10 times lower ^{220}Rn production than the sand used in the experiments, groundwater extraction with a rate of 11 L/min from a 2'' extraction well with screen length of 1 m is expected to produce a ^{220}Rn concentration of about 0.7 Bq/L in the water close to the well. Even if the decay of ^{220}Rn during transport to the detection system is neglected, the estimated ^{220}Rn concentration is lower than the system's ^{220}Rn -in-water detection limit.

Therefore we conclude that under common natural conditions (with respect to ^{220}Rn activity of the aquifer material, pumping rate, extraction well diameter and screen size, etc.) it is hardly possible to build up enough groundwater flow velocity to stimulate the emanation of ^{220}Rn . However, in pipes, the combination of radium-containing coatings and fast and turbulent flow conditions can indeed result in detectable ^{220}Rn concentrations (e.g. Burnett et al. (2007); Huxol et al. (2012)).

4.4 Summary and conclusion

To assess why the long lived ^{222}Rn (half-life 3.8 d) can be determined in soil gas and groundwater, but the short lived ^{220}Rn (half-life 55.6 sec) only in soil gas, we carried out two different laboratory experiments. The ^{220}Rn emanation to the gas phase was studied in a sandbox by simulating changing water contents of a soil column. The influence of different groundwater flow velocities on the ^{220}Rn -in-water concentrations was studied by extracting water from the fully saturated sandbox and from a flow tank. The use of a ^{220}Rn -active sand and an experimental set-up to significantly enhance the groundwater flow-velocity allowed us to determine ^{220}Rn in both, the gas and water phase under changing water contents and different flow conditions. The achieved results enabled us to identify the general mechanisms and processes that constrain the occurrence of ^{220}Rn in the gas and water phase of natural porous media.

- In partially saturated porous media, the migration of ^{220}Rn through the pore space and therefore the concentration of ^{220}Rn in the gas phase is limited due to the abundance of water menisci.
- Under saturated conditions, the ^{220}Rn -in-water concentrations depend on the induced shear stress on immobile water layers around aquifer grains and therefore on the groundwater flow velocity. Hence, it is concluded that high flow-velocities are able to disturb water layers around the grains and enlarge the sampling volume from which ^{220}Rn is extracted.

From these findings we draw the following general conclusions for subsurface fluid and solutes. In partially saturated media, water considerably influences the migration not only of ^{220}Rn , but also of any other soil gas species. The enhanced abundance of water menisci reduces the permeability of soils, as the soil gas species have to pass through more water-filled space by diffusion. Hence, water menisci increase the tortuosity of porous media for gas phase transport and therefore reduce the effective diffusion coefficient of gases in soil.

As shown by our experiments in the saturated sandbox and the tank, the concentrations of ^{220}Rn , and hence of other solutes can depend on the groundwater flow velocities, especially in cases when the solute species is exchanged between the water phase and the mineral surfaces. Regarding groundwater sampling campaigns for such species it is therefore important to sample the extraction wells every time with the same pumping rate, i.e. to induce the same groundwater flow velocity towards the sampling well.

Acknowledgments

We thank Marian Furjak for the gamma-ray analysis of the used sand. Heinz Surbeck and Eduard Hoehn are thanked for their helpful comments and the fruitful discussions. We thank Thomas Stieglitz and Fedora Quattrocchi for reviewing and improving our manuscript. This work was financed by the Swiss National Science Foundation (SNF-projects 200021-119802 and 200020-135513)

4.5 Annex 1: Sand properties

4.5.1 Emanation coefficient

The emanation coefficient of the sand was determined for both radon isotopes. 3 kg of air-dried sand were stored in a closed vessel of about 11 L volume for about 4 weeks to allow ^{222}Rn to reach its secular equilibrium. Subsequently, the air in the vessel was analyzed with a RAD7 for the ^{220}Rn and ^{222}Rn activity. The emanation coefficient E was calculated by

$$E = \frac{C_{\text{Rn}} * V_{\text{air}}}{A_{\text{Ra}} * M_{\text{sand}}} \quad (4.1)$$

whereas C_{Rn} is the measured radon isotope concentration (Bq/m^3), V_{air} is the volume of air in the closed vessel and the RAD7 (m^3), A_{Ra} is the radium isotope activity, determined by gamma spectroscopy in a germanium well detector (Bq/kg), and M_{sand} is the mass of the sand (kg).

For both radon isotopes the emanation coefficient was found to be ~ 0.1 .

4.5.2 Soil water characteristic curve

The soil water characteristic curve describes the amount of water that retains in a soil for a given matrix potential, e.g. capillary force. For the used sand, the soil water characteristic curve was determined in a pressure chamber. In the chamber,

four samples of water saturated sand were arranged on a water saturated porous plate. The pressure in the chamber was increased stepwise from 0 to 345 cmH₂O. After each increase, the loss of water from the sand samples was determined by weighing. The water retention curve of the sand (Figure 4.7) reflect the mean of the four samples and shows a typical sand-texture shape (Tuller and Or, 2005).

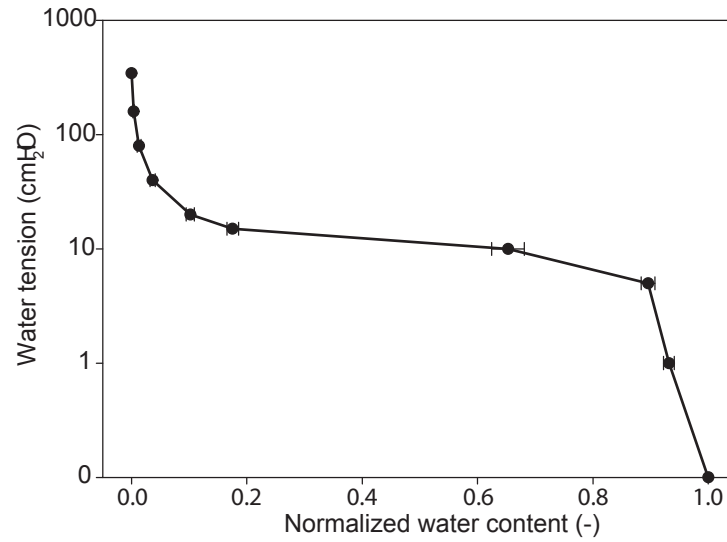


Figure 4.7: Soil water characteristic curve of the sand used in the laboratory experiments for fillin the sandbox and the tank.

Chapter 5

The different behavior of ^{220}Rn and ^{222}Rn in soil gas transport processes and its application

This chapter is in preparation in collaboration with Matthias S. Brennwald, Ruth Henneberger and Rolf Kipfer for publication in Environmental Science and Technology.

Abstract Radon (Rn) is a naturally occurring radioactive noble gas, which is ubiquitous in soil gas. Especially its long-lived isotope ^{222}Rn (half-life: 3.82 d) gained widespread acceptance as a tracer for gas transport in soils, while the short-lived ^{220}Rn (half-life: 55.6 s) found less interest in environmental studies. However, in some cases, the application of ^{222}Rn as a tracer in soil gas is complex as its concentrations can be influenced by changes of the transport conditions or of the ^{222}Rn activity of the soil material. Due to the different half-lives of ^{220}Rn and ^{222}Rn , the lengths that can be passed by the respective isotopes before decay differ significantly and ^{220}Rn migrates over much shorter distances than ^{222}Rn . Therefore, the concentrations of ^{220}Rn and ^{222}Rn are influenced by processes on different length scales. In laboratory experiments in a sandbox, we studied the different transport behaviors of ^{220}Rn and ^{222}Rn resulting from changing the boundary conditions for diffusive transport and from inducing advective gas movements. From the results gained in the laboratory experiments we propose the combined analysis of ^{220}Rn and ^{222}Rn to determine gas transport processes in soils. In a field study on soil gases in the cover soil of an old landfill we firstly showed the benefit of the combined analysis of ^{220}Rn and ^{222}Rn in soil gas.

5.1 Introduction

Radon (Rn) is a naturally occurring radioactive noble gas. The most abundant natural isotopes are ^{222}Rn (half-life 3.82 d) and ^{220}Rn (half-life 55.6 s). Both isotopes are generated by alpha decay of their specific precursor isotopes of radium. As noble gas, radon isotopes are released from radium bearing solid soil grains to soil gas (Nazaroff, 1992).

The abundance of the long-lived radon isotope ^{222}Rn in soil gas has been extensively applied to study processes related to gas fluxes in soils. To study the diffusivity of gases in soils and the soil gas transport, ^{222}Rn -concentrations in depth profile were determined (Dörr and Münnich, 1990; Lehmann et al., 2000). By using ^{222}Rn concentrations to derive parameters for vertical diffusion and exhalation, the fluxes and metabolism of reactive gases such as CO_2 , N_2O and CH_4 have been studied (Born et al., 1990; Uchida et al., 1997; Dueñas et al., 1999; Conen et al., 2002; Schroth et al., 2012).

In contrast, until today, the short-lived ^{220}Rn found less interest in environmental science. Nevertheless, ^{220}Rn has been used to assess gas fluxes near the ground (Lehmann et al., 1999, 2001). In combination with ^{222}Rn and CO_2 , ^{220}Rn was used to determine the origin and to quantify the transport of fumarole gases at Mount Etna (Giammanco et al., 2007).

However, often soil gas fluxes cannot solely be described by vertical gas diffusion. For instance in the cover soil of landfills where gases are produced by decomposing wastes and lateral gas fluxes exist, soil gas transport can be controlled by advective gas migration in all three dimensions (Christophersen and Kjeldsen, 2001; Franzidis et al., 2008). Due to its long half-life, ^{222}Rn migrates in the soil's pore space before decay. Therefore, the ^{222}Rn concentration in such soils can be influenced by soil gas movements and lateral mixing with soil gas from other sources. In addition, also changes in the ^{222}Rn source strength of the soil material can influence the ^{222}Rn concentration (Dörr and Münnich, 1990). In these cases, ^{222}Rn concentration profiles are complex to interpret and not useful as measure for diffusive soil gas fluxes.

Due to its much shorter half-life, ^{220}Rn migrates over much shorter distances than the long-lived ^{222}Rn . Therefore, ^{220}Rn concentrations in soil gas only reflect the very local conditions of the soil. Addressing this knowledge, we propose the combined analysis of ^{220}Rn and ^{222}Rn concentrations in soil gas profile to determine the disturbing influence on ^{222}Rn concentration profiles. In this paper we present the results of laboratory experiments in a sandbox, assessing the different transport behavior of ^{220}Rn and ^{222}Rn under different gas flux conditions. Subsequently, we apply the findings of the laboratory experiments to analyze and interpret a concentration profile of ^{220}Rn and ^{222}Rn , and of the reactive gases O_2 , CO_2 and CH_4 in a cover soil of a landfill.

5.2 Material and methods

All radon isotope concentration measurements were conducted with the radon analyzer Rad7 (DurrIDGE Company, Inc). In the instrument's "sniff" mode, the internal pump of the radon analyzer runs continuously and the concentrations of ^{220}Rn and ^{222}Rn are determined simultaneously by measuring the alpha decay of their respective daughters, ^{216}Po and ^{218}Po . Depending on the half-life of the respective polonium isotope, the ^{220}Rn concentration is determined after less than a second, whereas the ^{222}Rn concentration is determined after about 15 minutes.

5.2.1 Laboratory measurements

Sandbox

The sand and the sandbox used in the laboratory experiments have been described in detail elsewhere (Huxol et al., 2013). In short, the sand material consists of grains that are coated with manganese oxide. In a technical purification process of anoxic mineral water, the material was enriched with radium isotopes. The sand is therefore an exceptionally strong source of radon isotopes. The closable sandbox (length 119 cm, height 95 cm, depth 16 cm) was filled up to 75 cm with sand, leaving an air space of 20 cm above the sand (Figure 5.1). To attain a homogeneous distribution of the sand, the box was filled with water-saturated sand. After filling, the sand was allowed to dry and to equilibrate for ^{222}Rn for four weeks. The bottom of the sandbox consists of a perforated metal sheet, covered with a 250 μm PVC-mesh. The space below the metal sheet is connected to supply pipes on both sides of the sandbox. To the supply pipes, a membrane pump was connected to induce advective gas fluxes from bottom to top.

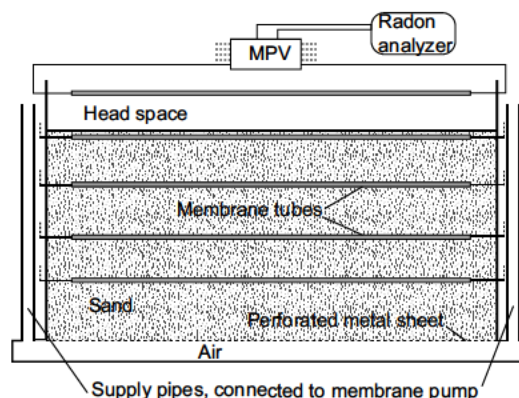


Figure 5.1: Sandbox used in laboratory experiments. Membrane tubes for gas sampling are connected in distinct loops (explicitly shown for membrane tube in the head space of the sandbox) to the multiposition valve (MPV). Membrane pump to inject air through supply pipes is not shown.

To sample radon isotopes from the sandbox, polypropylene membrane tubes (Accurel® PP V8/2) of 1 m length were installed horizontally, four in the sand in the depth of 1, 9, 24, and 44 cm, and one in the head space 16 cm above the sand. All membrane tubes were connected in distinct loops with PVC tubes via an automatic multiposition valve (MPV) to the RAD7 radon analyzer. The internal pump of the RAD7 was used to circulate the sampled gas between a selected membrane tube and the radon analyzer. Sensors (5TE, Decagon Devices Inc.) at each sampling depth measured the water content of the sand.

The MPV was programmed to switch hourly between the different sampling depths to be analyzed. To avoid memory effects of the radon analyzer, the analyzer was purged with virtually radon-free ambient air after analysis of all sampling depths for one hour. Hence, each depth was analyzed four times a day for one hour, yielding four hourly mean radon isotope concentrations per depth and day.

Experimental work

To analyze the migration dynamics of ^{220}Rn and ^{222}Rn in respect to purely diffusive exchange (A), and to advective-diffusive transport (B), we conducted the following experiments:

A. Diffusive exchange in a open/closed sandbox In this experiment we did not use the membrane pump and the supply pipes were closed. In a first step, we measured the radon isotope concentrations during 2 days from the open box, i.e. the radon isotopes were allowed to escape from the sandbox. In a second step, we closed the sandbox with a lid to change the boundary conditions for diffusive transport. After 5 days, we opened it to re-establish the initial steady-state condition.

B. Advective-diffusive flow through the box In this experiment, we pumped virtually radon-free ambient air via the supply pipes from bottom to top through the open sandbox. The induced air flow rates through the sand were 2, 4, and 6 L/min. Between each increase of the pumping rate, the sandbox was left for at least 30 h to re-establish the steady-state condition.

Diffusion model

To determine the effective diffusion coefficient of radon in the sand, we modeled the distribution of the radon isotope concentrations in the open, undisturbed sandbox. As the sampling tubes integrate over almost the whole length of the sandbox, we considered the diffusive transport of the radon isotopes towards the sand/atmosphere interface as a one-dimensional process. The air exchange above

the sand was limited and the radon isotope concentrations in the head space of the sandbox could not be assumed to be zero. Therefore, the well known analytical solution describing the radon isotope concentration distribution with depth ($C(z)$ in Equation 5.1; Nazaroff, 1992) was extended with a term B for the radon isotope concentration in the head space:

$$C(z) = C_{\infty}(1 - e^{-z/l}) + B(e^{-z/l}) \quad (5.1)$$

whereas C_{∞} is the radon isotope equilibrium concentration (Bq/m^3), z is the depth (m), directed downwards from the soil surface, and l is the diffusion length of radon isotope (m). l is defined as $\sqrt{D_e/\lambda}$, whereas λ is the radon isotope specific decay constant ($1/\text{s}$) and D_e is the effective diffusion coefficient (m^2/s), assumed to be equal for both radon isotopes. l describes the length after which the initial radon concentration is reduced to $1/e$.

For modeling concentration profile of ^{220}Rn and ^{222}Rn in the sandbox, we applied Equation 5.1 simultaneously for both radon isotopes. We fitted the modeled radon isotope concentrations to the measured concentrations by varying the effective diffusion coefficient D_e , the respective radon isotopes equilibrium concentration C_{∞} and, for the ^{222}Rn -concentration profile the concentration in the head space B by minimizing the sum of the normalized individual deviations. This process was iteratively repeated until optimum agreement between the measured and the modeled radon isotope concentrations. In addition, we carried out Monte Carlo simulations to determine the uncertainty of the fitted parameters.

Pressure differences

We converted the applied air flows Q through the sandbox (2, 4 and 6 L/min) to pressure differences between sandbox and ambient air δP by using Darcy's law, which is also valid for unsaturated porous media (Scanlon et al., 2002):

$$\frac{\delta P}{\delta z} = \frac{Q}{A} \frac{\nu_{\text{air}}}{k} \quad (5.2)$$

where δz is the length of the sand column (m), A is the cross sectional area (m^2) of the sandbox, ν_{air} is the dynamic viscosity of air ($\text{Pa}\cdot\text{s}$) and k is the intrinsic permeability (m^2). k was approximated via

$$k = \frac{K_w \mu_w}{\rho_w g} \quad (5.3)$$

where μ_w is the dynamic viscosity of water ($10^{-3} \text{ Pa}\cdot\text{s}$ at 20°C), ρ_w is the density of water (1000 kg/m^3), g is the gravitational acceleration (9.81 m/s^2), and K_w is the hydraulic conductivity of the sand material in the box for water at 20°C and

density of 1000 kg/m^3 (10^{-4} m/s). K_w was approximated by the empiric formula of Hazen (1892):

$$K_w = 0.0116 \times d_{10}^2 \quad (5.4)$$

where d_{10} is the grain diameter of the sand at 10 % weight portion, (0.1 mm, from Huxol et al. (2013)).

As a result, the induced pressure differences δP are 24 Pa, 48 Pa and 72 Pa, which are well in the range of measured pressure differences between the gas phase of landfill and the atmosphere (Christophersen and Kjeldsen, 2001). Therefore, laboratory finding on the behavior of the ^{220}Rn and ^{222}Rn concentrations in response to advective air flow can be assumed to be representative for the conditions in landfills

5.2.2 Field measurements

Field site

To evaluate the application of the combined analysis of ^{220}Rn and ^{222}Rn under field conditions, we determined the radon isotope concentrations in a vertical profile in the cover soil of a closed landfill. The landfill is located in the northwest of Switzerland, near the city of Liestal, 570 m above sea level at the highest point. Opened in 1949, the 12.3 ha landfill received ca. $3.2 \times 10^6 \text{ m}^3$ of household, office construction and industrial waste. The landfill was closed in 1994 and subsequently covered with a 2.0-2.5 m thick heterogeneous mixture of sandy-loam, pebbles, rocks, boulders, and construction material. The total porosity of the cover soil is estimated to be ~ 0.5 (Gómez et al., 2009). The soil is now covered by a mixed, intermittent vegetation consisting of grass, small trees and shrubs. To monitor the gas emission from the landfill soil-gas sampling tubes are installed in the cover soil of the landfill arranged in vertical profile in several locations.

Sampling

The sampled profile instrumentation consists of stainless steel extraction needles of 1.5 mm diameter, reaching down to 0.15, 0.4, 0.6 and 0.95 m depth (for installation details see Gómez et al., 2009). In addition, we installed another stainless steel needle to extract soil gas from the depth of 0.02 m.

We started the analysis for ^{220}Rn and ^{222}Rn in the soil gas profile at the lowest sampling depth of 0.95 m and continued subsequently with the next higher sampling depths. While extracting the soil gas for 5 min by a rate of approx. 0.7 L/min by using the radon analyzers internal pump, the soil gas ^{220}Rn concentration was determined. After extraction, the internal pump was stopped and the inlet and

outlet of the radon analyzer were closed with compression valves. Subsequently, the radon analyzer was allowed to attain a secular equilibrium of the ^{218}Po activity for 15 min before analyzing the ^{222}Rn concentration for 20 min. Prior to the analysis of the next soil gas batch, the radon analyzer was purged for at least 5 min with virtually radon isotope free ambient air to avoid memory effects in the radon analyzer.

The radon isotope measurements at the old landfill were combined with a regular monitor campaign on reactive soil gases. Sample collection and analysis of soil gas for CH_4 , CO_2 and O_2 was done as described previously (Henneberger et al., 2012). The soil gas sampling was done during a period of dry weather, causing a dry top-layer of the soil (referred as “dry conditions”). After 8 days, in which about 30 mm rain precipitated (“wet conditions”), we repeated the radon isotope measurements only (no other gases were measured).

5.3 Results and discussion

5.3.1 A. Diffusion

In the open, undisturbed sandbox, both the ^{222}Rn and the ^{220}Rn concentrations increased with depth (Figure 5.2, solid lines). The ^{222}Rn concentration increased approximately linearly with depth of the sandbox and did not attain a secular equilibrium concentration between radioactive production and decay. The ^{220}Rn concentration, however, reached its secular equilibrium concentration of about 90 kBq/m^3 in the sampling depth of 9 cm, and did not change significantly below this depth. After having closed the sandbox for 5 days, the ^{222}Rn concentrations in all sampling depths increased and converged to concentrations between $21.5\text{--}24.2 \text{ kBq/m}^3$. After opening of the sandbox, the ^{222}Rn concentrations profile returned to the initial profile. The ^{220}Rn concentration profile however, did not change significantly during the experiment (Figure 5.2, right, and Figure 5.3).

The different behavior of the two radon isotopes can be understood by their different diffusion lengths, resulting from the different half-lives of ^{222}Rn and ^{220}Rn . By fitting modeled radon isotope concentration profile to the observed concentrations, we determined the effective diffusion coefficient to be $(7.7 \pm 1.1) \times 10^{-6} \text{ m}^2/\text{s}$. This agrees with an effective diffusion coefficient of $(7.0 \pm 0.1) \times 10^{-6} \text{ m}^2/\text{s}$, derived in a similar experiment (Van Der Spoel et al., 1997). The resulting specific isotope diffusion lengths are of $1.91 \pm 0.13 \text{ m}$ for ^{222}Rn and $0.025 \pm 0.002 \text{ m}$ for ^{220}Rn . As the diffusion length of ^{222}Rn is considerably larger than the total height of the sandbox, ^{222}Rn from all depths can escape from the sandbox. Therefore, ^{222}Rn did not reach the secular equilibrium concentration in the sandbox. In the closed sandbox, the lid prevented outgassing, which resulted

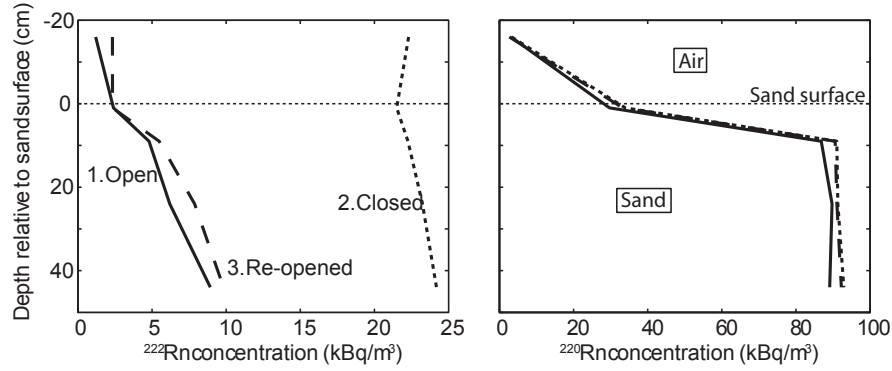


Figure 5.2: Depth profile of ^{222}Rn and ^{220}Rn from the open box (solid line), the closed box after five days of accumulation (dotted line) and re-opened box (dashed line).

in an accumulation of ^{222}Rn in the sandbox. In contrast, the diffusion length of ^{220}Rn is much shorter than the height of the head space. Therefore, ^{220}Rn was not able to escape, even from the open sandbox. Hence, the ^{220}Rn concentrations are independent from closing the sandbox and did not change over the whole period of the experiment.

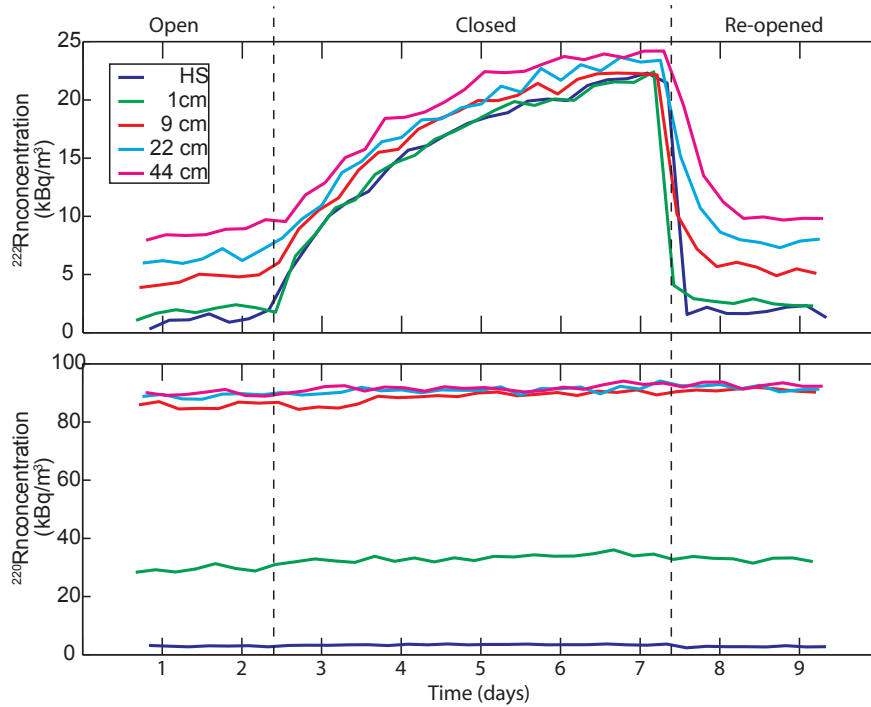


Figure 5.3: Concentrations of ^{222}Rn and ^{220}Rn in the head space (HS) and the different depths of the sandbox, measured in the open, closed and re-opened sandbox.

5.3.2 B. Advection

Before exerting air flow through the sandbox, the ^{222}Rn and ^{220}Rn concentrations showed the diffusion-controlled concentration profile known from the open sandbox. The slightly lower ^{220}Rn concentrations in the depths of 22 and 44 cm thereby reflect the slightly higher water contents in these particular depths ($0.11 \text{ m}^3/\text{m}^3$ versus $0.08 \text{ m}^3/\text{m}^3$ in 9 cm depth), as an increased soil water content limits the release of ^{220}Rn from the solid soil grains and therefore reduce the ^{220}Rn concentration in soil gas (Huxol et al., 2012).

The induced inflow of fresh air, however, affected the ^{222}Rn concentrations from all depths to converge to approx. 4 kBq/m^3 , independently of the applied pumping rate (Figure 5.4, top). Hence, all ^{222}Rn concentrations in depths $\geq 9 \text{ cm}$ decreased, while the ^{222}Rn concentration in the depth of 1 cm increased. The ^{222}Rn concentration in the head space was unaffected by the soil gas advection. In the periods with zero advection, the ^{222}Rn concentrations returned to the diffusion-controlled concentration profile

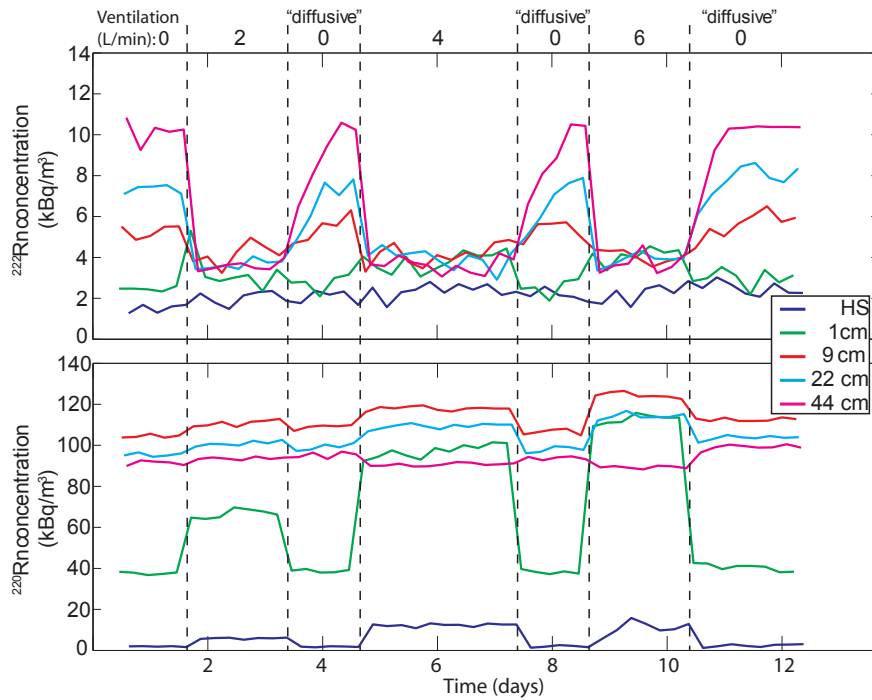


Figure 5.4: Concentrations of ^{220}Rn and ^{222}Rn in the head space (HS) and the different depths of the sandbox, while applying gas flows of 2, 4, and 6 L/min from bottom to top to the open sandbox.

The ^{220}Rn concentrations, however, showed a behavior which was different from that of ^{222}Rn . When exerting the air flow through the sandbox, the ^{220}Rn

concentrations increased at higher pumping rates, most obvious in the depth of 1 cm and in the head space (Figure 5.4, bottom). Only in the sampling depth of 44 cm, the ^{220}Rn concentrations decreased slightly at pumping rates of 4 and 6 L/min.

The different response of ^{222}Rn and ^{220}Rn to the applied air flows is again caused by their different half-lives and therefore different migration lengths. We calculated the mean travel time by using a migration length that considers advective and diffusive transport (Antonopoulos-Domis et al., 2009). At the lowest pumping rate of 2 L/min, the mean travel time of the introduced air to reach the uppermost sampling tube in the depth of 1 cm was approx. 70 min. This is only approx. 1% of the half-life of ^{222}Rn and therefore much too short to allow the ^{222}Rn concentration to significantly increase on the way from bottom to top. Therefore, also the differences of the transfer times between the different sampling depths are negligible, causing the ^{222}Rn concentrations of all sampling depths to converge to similar values throughout the sandbox.

In contrast, due to its short half-life, the ^{220}Rn concentrations in the introduced fresh air increase much faster and are able to reach the equilibrium concentration in all depths. Only at the lowermost sampling depth of 44 cm at the highest pumping rate, the mean travel time of about 10 min was short enough to slightly decrease the ^{220}Rn concentration. In the other depths, in contrast, the advective air flows even forced the ^{220}Rn concentrations to reach higher values than under diffusion-controlled transport. In the uppermost sampling depth of 1 cm, and in the open head space of the sandbox, this increase is caused by transport of ^{220}Rn -rich gas from lower depths. However, in the lower depths the diffusion-controlled ^{220}Rn concentrations are very similar and transport of ^{220}Rn -rich gas can therefore be excluded. Instead, it is more likely that the increase in ^{220}Rn concentrations was caused by the higher air flows themselves, most visibly at 9 cm. The effect of increased ^{220}Rn concentrations in response to higher flow velocities is known from fast flowing groundwater and is associated to enhanced shear stress (Huxol et al., 2013). The shear stress disturbs immobile water layers around the soil grains, which commonly constrain the release of ^{220}Rn from the minerals to the flowing water. In analogy to the situation under saturated conditions, we conclude that also in unsaturated porous media higher gas flow velocities reduce immobile gas film around the mineral grains, which in consequence allows more ^{220}Rn to reach the gas phase within the soil.

To summarize, the laboratory experiments showed that, due to the longer half-life and migration length, the ^{222}Rn concentrations integrate transport characteristics over larger distances than the ^{220}Rn concentrations. The ^{222}Rn concentrations can therefore be affected by changes influencing the diffusive gas transport. Also advectively transported fresh air influence the ^{222}Rn concentrations. The ^{220}Rn concentrations, in contrast, reflect only the very local characteristics and condi-

tions of the sand and are therefore much less affected by changes of the transport conditions. Acknowledging the different behavior of both radon isotopes to transport processes, we propose the simultaneous and combined analysis of ^{220}Rn and ^{222}Rn in soil gas profiles to analyze soil gas transport processes.

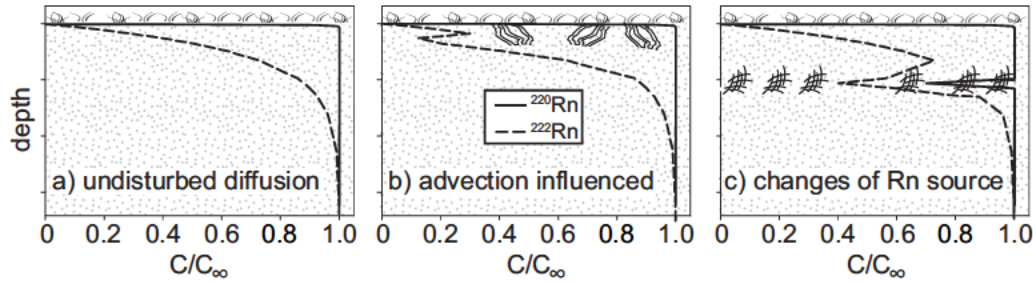


Figure 5.5: Theoretical radon isotope concentrations in a) undisturbed diffusion profile; b) profile influenced by air injections of different origin and age; and c) profile that is influenced by changes in the radon isotope source strength.

Hence, by comparing the concentration profiles of ^{220}Rn and ^{222}Rn , deviations of one or both radon isotopes from the ideal diffusion-controlled concentration profile (Figure 5.5a) can be associated with the different processes and conditions which can influence the ^{222}Rn concentration in a soil gas depth profile. For instance, the injection of fresh air will only affect the concentration profile of ^{222}Rn as ^{220}Rn reaches its equilibrium concentration very fast (Figure 5.5b). Changes of the local source strength of ^{220}Rn and ^{222}Rn , however, will result in deviations in the concentration profiles of both radon isotopes (Figure 5.5c).

5.3.3 Field results

To test the applicability of the combined and simultaneous determination under field conditions, we studied the concentrations of both radon isotopes in the cover soil of an old landfill combined with reactive gases, under dry and under wet weather conditions. Under dry conditions, ^{222}Rn in the soil depth profile (filled circles in Figure 5.6, left) showed variable concentrations with depth and would be complex to interpret without any additional data. However, by combining the ^{222}Rn concentrations with the ^{220}Rn concentrations (filled triangles), which were measured simultaneously, the gas transport processes in the soil can be better understood. The ^{220}Rn data indicates two different zones, one with higher production of ^{220}Rn in depths above 40 cm and one with lower production below that depth. However, on the 2-sigma error level (not shown), the ^{220}Rn concentration were rather constant below 15 cm, implying a rather constant radon isotope production throughout the profile. Therefore, the lower ^{222}Rn concentrations, at least in the depth of

40 cm, cannot be attributed to a local radon isotope source effect. The low ^{222}Rn concentration rather can be explained by the injection of ^{222}Rn -depleted air to this depth. Moreover, as the ^{222}Rn concentrations above and below the depth of 40 cm are higher, the source of the ^{222}Rn -depleted air is most probably related to lateral soil-gas injections, i.e. as advective gas input through highly permeable soil zones, such as cracks or macro pores. As shown in our laboratory experiments, increased gas flow-velocities enhance the ^{220}Rn release from the soil grains. Hence, the slightly increased ^{220}Rn concentration in the depth of 40 cm indicates advective soil gas movements at this depth, too.

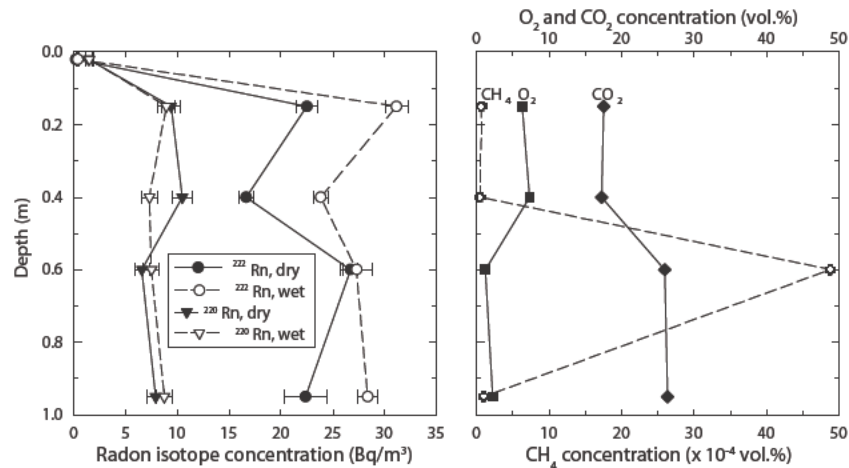


Figure 5.6: Radon isotope concentrations (left, error bars indicate 1-sigma error), and volumetric concentrations of CH₄, CO₂ and O₂ (right) measured in a soil gas profile of the landfills soil cover. Filled symbols indicate concentrations under dry soil top-layer conditions while open symbols the concentrations after a period of 8 days with about 30 mm precipitation and hence wet top-layer of soil. Samples for the reactive gases were taken immediately before the radon isotope concentration measurements under dry conditions.

Under wet conditions, the radon isotope concentrations support our interpretation of the ongoing processes in the soil profile. With exceptions in the depths of 2 and 60 cm, all ^{222}Rn concentrations (open circles in Figure 5.6, left) were substantially increased compared to the ^{222}Rn concentrations measured under dry conditions. This behavior is explained by the changed transport conditions of the soil. The rain increased the soil water content of the soil surface. As a consequence, clogging of the soil pores in the top-layer with water reduced the gas exchange with the atmosphere, which led to the accumulation of ^{222}Rn in the soil gas (Schery et al., 1984; Nazaroff, 1992).

The ^{220}Rn concentrations profile measured under wet conditions (open triangles), with exception in the depth of 40 cm, showed no significant changes. Hence, due to its shorter migration length, ^{220}Rn was not affected by the clogging of the

top-layer of the soil. The ^{220}Rn concentrations in 40 cm, however, decreased to a level equivalent to the ^{220}Rn concentrations in the other depths. This supports the assumed constant radon isotope production throughout the soil profile and indicates that the advective gas injections found under dry conditions in this depth were reduced by the clogging of the soils top-layer.

The soil gas concentrations of the reactive gases measured under dry conditions are shown in Figure 5.6, right. Being compared to atmospheric conditions (Hites and Raff, 2012), throughout the whole profile the O_2 concentrations (filled squares) in soil gas were strongly depleted, whereas the CO_2 concentrations (filled diamonds) were strongly increased. The depletion of O_2 and the increase of CO_2 was intensified below the depth of 40 cm. Together with the concentration pattern of ^{220}Rn under dry conditions, this indicates structural differences between these layers.

With exception of the concentration peak in the depth of 60 cm, the CH_4 concentrations (filled crosses) in the soil gas profile were similar, or even slightly reduced, compared to atmospheric conditions. However, even the peak concentration in the depth of 60 cm with about 50 ppm was approx. 3 orders of magnitude lower than typical CH_4 concentrations produced from landfill (Farquhar and Rovers, 1973). Together with the unchanged ^{222}Rn concentrations in this depth under dry and wet conditions, the results indicate that the soil gas in this depth is decoupled and therefore undisturbed by any external influence. However, over the entire profile and in general, the concentrations of O_2 and CH_4 were depleted and the concentrations of CO_2 were increased. This implies that this particular soil profile acted on that particular day under dry conditions as CH_4 -sink. The radon isotope concentrations strengthen this interpretation by indicating (probably advective) influence of fresh, ^{222}Rn depleted air. However, when using needles for soil gas extraction, leakage may occur along the needle. Therefore, the soil gas sampled with the needles might be influenced and diluted by outside air.

By applying the knowledge gained in the laboratory to the field we demonstrated that the simultaneous determination of ^{220}Rn and ^{222}Rn strengthens the understanding of soil gas transport processes in porous media. In the presented case, the exclusive use of ^{222}Rn as soil gas tracer would not allow solid interpretation of the transport processes. The combined analysis of ^{220}Rn and ^{222}Rn , however, allowed us to conclude that at least some depths of the studied soil depth profile were influenced by advectively injected fresh air. As the interpretation of the radon data can be complex, more knowledge and experience in the combined analysis of radon isotopes is needed. Nevertheless, the results presented here are a first step in establishing ^{220}Rn as (co-)tracer for soil-gas transport process measurements in the unsaturated zone.

Acknowledgments

We thank the Swiss National Science Foundation for funding this project (SNF projects 200021-119802 and 200020-135513).

Chapter 6

Synthesis and outlook

This thesis proposes the short lived radon isotope ^{220}Rn as a tracer for short-term and small-scale processes in subsurface systems as groundwater and soil gas. Due to its short half-life of 55.6 sec, the sampling and analysis procedure for ^{220}Rn concentrations in water is challenging and had to be optimized. Therefore, the first goal of the thesis was to develop a fast, reliable and robust measurement protocol for the ^{220}Rn -in-water detection. This goal was successfully completed and the feasibility of ^{220}Rn -in-water detection was proven in laboratory experiments. Subsequently, the measurement system was applied to the field testing various aquifer systems for ^{220}Rn . However, no significant ^{220}Rn concentrations could be detected in natural groundwater, although ^{222}Rn was detectable in all tested systems. However, in contrast to groundwater, in soil gas ^{220}Rn is ubiquitously detectable (Nazaroff, 1992).

Field and laboratory experiments under unsaturated and saturated conditions to study the emanation and migration characteristics of ^{220}Rn revealed that immobile water phases act as barriers for the ^{220}Rn release and transport in the subsurface. Due to its short half-life, ^{220}Rn decays while passing these barriers diffusively. Hence, under partially saturated conditions, water films inhibit the release of ^{220}Rn from the soil grains to the gas-filled pore space, in which water menisci between the soil grains further constrain the migration of ^{220}Rn . Therefore, if the water content reaches a critical, soil-specific threshold, the ^{220}Rn concentration in soil gas gets reduced to virtually zero. Under fully saturated conditions, ^{220}Rn decays in immobile water layers around the grains before it can reach the moving water phase. In targeted laboratory experiments, however, it was found that fast flow velocities produce shear stress on the water layers. This shear stress reduces the immobile water layers in thickness and stimulates the release of ^{220}Rn from the soil grains to the fast flowing water. However, in common natural aquifers and with common groundwater pumping rates and sampling techniques, it is probably not possible to induce enough groundwater flow velocity to stimulate the release of

^{220}Rn , which can therefore not be measured.

However, the results of the thesis showed that concentrations of ^{220}Rn in soil gas still are a promising tracer in the unsaturated zone, especially in combination with the long-lived radon isotope ^{222}Rn . In contrast to ^{222}Rn , the ^{220}Rn concentrations in soil gas are much less influenced by soil gas transport processes. Therefore, especially in soils that are influenced by advective soil gas movements the analysis and interpretation of ^{222}Rn concentrations is complicated and can be ambiguous. The combined analysis of both radon isotopes allows to draw conclusions on the soil gas transport processes. This knowledge strengthens the interpretations about reactive soil gases, too.

Overall, this thesis gives explanations why ^{220}Rn is detectable in soil gas but not in groundwater. The initial aim to establish ^{220}Rn as a tracer in aquatic systems could not be completed because its short half-life and, therefore, short migration length in the water phase. But, as now the mechanistic basis of the ^{220}Rn emanation from subsurface materials is known, an improved technical attempt might be successful in the detection of ^{220}Rn from groundwater. Also, as the determination of ^{220}Rn in soil gas is relatively simple, the application of ^{220}Rn in this environment should be stronger emphasized. To complete these goals, the following tasks are formulated:

Task I: Establish ^{220}Rn as tracer in soil gas The thesis showed the promising benefit of the use of ^{220}Rn in the unsaturated zone. Especially, when the ^{222}Rn measurements show inconsistent results, the analysis of ^{220}Rn can improve the interpretation of the soil gas data. With the used radon detector RAD7, the combined analysis of ^{220}Rn and ^{222}Rn concentrations in soil gas is feasible with only little rearrangement of the sampling and measuring protocol that is routine for ^{222}Rn measurements. However, more knowledge and experience is needed to establish ^{220}Rn as (co-)tracer in the unsaturated zone. Therefore, ^{220}Rn should be included in future field campaigns on ^{222}Rn measurement in soil gas.

Task II: Technical improvement of groundwater sampling for ^{220}Rn As demonstrated in the thesis, the groundwater flow velocities induced with common groundwater extraction methods are too slow to stimulate the release of ^{220}Rn from the aquifer grains to the moving water. Therefore, the development of technical facilities to increase the flow velocities towards the sampling wells have to be targeted. To do so, a packer system, combined with an integrated groundwater pump should be designed. With such a system, smaller sections of the well's screen can be separated to reduce the surface area and apply stronger extraction rates. This attempt might produce more shear stress on the aquifer grains in the vicinity of the extraction well to eventually detect significant ^{220}Rn -in-water concentrations.

Bibliography

- Adler, P. M. and Perrier, F. (2009). Radon emanation in partially saturated porous media. *Transport in Porous Media*, 78(2):149–159.
- Andrews, J. N. and Wood, D. F. (1972). Mechanism of radon release in rock matrices and entry into groundwaters. *Trans. Inst. Mining Metall.*, Sect. B 81:B198–B209.
- Anthony, J., Bideaux, R., Bladh, K., and M.C, N. (2003). *Handbook of mineralogy*. Mineralogical Society of America, Chantilly, VA 20151-1110. <http://www.handbookofmineralogy.org/>.
- Antonopoulos-Domis, M., Xanthos, S., Clouvas, A., and Alifrangis, D. (2009). Experimental and theoretical study of radon distribution in soil. *Health Physics*, 97(4):322–331.
- Bertin, C. and Bourg, A. C. M. (1994). Rn-222 and chloride as natural tracers of the infiltration of river water into an alluvial aquifer in which there is significant river groundwater mixing. *Environmental Science & Technology*, 28(5):794–798.
- Binder, H. H. (1999). *Lexikon der chemischen Elemente: Das Periodensystem in Fakten, Zahlen und Daten*. S. Hirzel.
- Born, M., Dörr, H., and Levin, I. (1990). Methane consumption in aerated soils of the temperate zone. *Tellus B*, 42(1):2–8.
- Bossus, D. A. W. (1984). Emanating power and specific surface area. *Radiation Protection Dosimetry*, 7(1-4):73–6.
- Burnett, W. C., Dimova, N., Dulaiova, H., Lane-Smith, D., Parsa, B., and Szabo, Z. (2007). Measuring thoron (^{220}Rn) in natural waters. In Warwick, P., editor, *Environmental Radiochemical Analysis III*, pages 24–37. RSC Publishing, Cambridge.

- Burnett, W. C. and Dulaiova, H. (2003). Estimating the dynamics of groundwater input into the coastal zone via continuous radon-222 measurements. *Journal of Environmental Radioactivity*, 69(1-2):21–35.
- Cable, J. E., Burnett, W. C., Chanton, J. P., and Weatherly, G. L. (1996). Estimating groundwater discharge into the northeastern Gulf of Mexico using radon-222. *Earth and Planetary Science Letters*, 144(3-4):591–604.
- Cartwright, I., Hofmann, H., Sirianos, M., Weaver, T., and Simmons, C. (2011). Geochemical and ^{222}Rn constraints on baseflow to the Murray River, Australia, and timescales for the decay of low-salinity groundwater lenses. *Journal of Hydrology*, 405(3-4):333–343.
- Christophersen, M. and Kjeldsen, P. (2001). Lateral gas transport in soil adjacent to an old landfill: factors governing gas migration. *Waste Management & Research*, 19(6):579–594.
- Clever, H. L. and Battino, R. (1979). *Krypton, xenon, and radon: gas solubilities*. Pergamon Press, Oxford; New York.
- Committee on the Biological Effects of Ionizing Radiations, National Research Council (1988). *Health Risks of Radon and Other Internally Deposited Alpha-Emitters: BEIR IV*. The National Academies Press.
- Conen, F., Neftel, A., Schmid, M., and Lehmann, B. E. (2002). $\text{N}_2\text{O}/^{220}\text{Rn}$ - soil flux calibration in the stable nocturnal surface layer. *Geophysical Research Letters*, 29(2):1025.
- Debiere, A.-L. (1900). Sur un nouvel élément radio-actif: l'actinium. *Comptes rendus hebdomadaires des séances de l'Académie des sciences*, 130:906–908.
- Dimova, N., Burnett, W., and Speer, K. (2011). A natural tracer investigation of the hydrological regime of Spring Creek Springs, the largest submarine spring system in Florida. *Continental Shelf Research*, 31(6):731–738.
- Dimova, N., Burnett, W. C., and Lane-Smith, D. (2009). Improved automated analysis of radon (^{222}Rn) and thoron (^{220}Rn) in natural waters. *Environmental Science & Technology*, 43(22):8599–8603.
- Dimova, N. T. and Burnett, W. C. (2011a). Evaluation of groundwater discharge into small lakes based on the temporal distribution of radon-222. *Limnology and Oceanography*, 56(2):486–494.

- Dimova, N. T. and Burnett, W. C. (2011b). Evaluation of groundwater discharge into small lakes based on the temporal distribution of radon-222. *Limnology and Oceanography*, 56(2):486–494.
- Dorn, E. (1900). Über die von radioactiven Substanzen ausgesandte Emanation. *Abhandlungen der Naturforschenden Gesellschaft zu Halle*, 23:2–15.
- Dörr, H. and Münnich, K. O. (1990). ^{222}Rn flux and soil air concentration profile in West-Germany. Soil ^{222}Rn as tracer for gas transport in the unsaturated soil zone. *Tellus B*, 42(1):20–28.
- Dueñas, C., Fernández, M. C., Carretero, J., and Liger, E. (1999). Methane and carbon dioxide fluxes in soils evaluated by ^{222}Rn flux and soil air concentration profiles. *Atmospheric Environment*, 33(27):4495–4502.
- Ekström, L. P. and Firestone, R. B. (2004). WWW Table of radioactive isotopes, database version 2/28/99 from URL <http://ie.lbl.gov/toi/index.htm>.
- Farquhar, G. J. and Rovers, F. A. (1973). Gas production during refuse decomposition. *Water, Air, & Soil Pollution*, 2(4):483–495.
- Fisher, E. L., Fuortes, L. J., Ledolter, J., Steck, D. J., and Field, R. W. (1998). Temporal and spatial variation of waterborne point-of-use Rn-222 in three water distribution systems. *Health Physics*, 74(2):242–248.
- Franke, A., Reiner, L., Pratzel, H. G., Franke, T., and Resch, K. L. (2000). Long-term efficacy of radon spa therapy in rheumatoid arthritis - a randomized, sham-controlled study and follow-up. *Rheumatology*, 39(8):894–902.
- Franzidis, J. P., Heroux, M., Nastev, M., and Guy, C. (2008). Lateral migration and offsite surface emission of landfill gas at City of Montreal landfill site. *Waste Management & Research*, 26(2):121–131.
- Freeze, R. A. and Cherry, J. A. (1979). *Groundwater*. Prentice Hall, New York.
- Fujiyoshi, R., Haraki, Y., Sumiyoshi, T., Amano, H., Kobal, I., and Vaupotic, J. (2010). Tracing the sources of gaseous components (^{220}Rn , CO_2 and its carbon isotopes) in soil air under a cool-deciduous stand in Sapporo, Japan. *Environmental Geochemistry and Health*, 32(1):73–82.
- Gainon, F., Goldscheider, N., and Surbeck, H. (2007). Conceptual model for the origin of high radon levels in spring waters - the example of the St. Placidus spring, Grisons, Swiss Alps. *Swiss Journal of Geosciences*, 100(2):251–262.

- Giammanco, S., Sims, K. W. W., and Neri, M. (2007). Measurements of ^{220}Rn and ^{222}Rn and CO_2 emissions in soil and fumarole gases on Mt. Etna volcano (Italy): Implications for gas transport and shallow ground fracture. *Geochemistry Geophysics Geosystems*, 8. Q10001.
- Gómez, K. E., Gonzalez-Gil, G., Lazzaro, A., and Schroth, M. H. (2009). Quantifying methane oxidation in a landfill-cover soil by gas push-pull tests. *Waste Management*, 29(9):2518–2526.
- Greeman, D. J. and Rose, A. W. (1996). Factors controlling the emanation of radon and thoron in soils of the eastern USA. *Chemical Geology*, 129(1-2):1–14.
- Härting, F. and Hesse, W. (1879). Der Lungenkrebs, die Bergkrankheit der Schneeberger Gruben. *Vierteljahrsschrift für Gerichtliche Medizin und Öffentliches Sanitätswesen*, pages 30: 296–309; 31: 102–132, 313–337.
- Hazen, A. (1892). Some physical properties of sands and gravels, with special reference to their use in filtration 24th annual report, Massachusetts State Board of Health. Pub.Doc. No.34, 539-556.
- Henneberger, R., Lüke, C., Mosberger, L., and Schroth, M. H. (2012). Structure and function of methanotrophic communities in a landfill-cover soil. *FEMS Microbiology Ecology*, 81(1):52–65.
- Hirsch, A. I. (2007). On using radon-222 and CO_2 to calculate regional-scale CO_2 fluxes. *Atmospheric Chemistry and Physics*, 7(14):3737–3747.
- Hirst, W. and Harrison, G. E. (1939). The diffusion of radon gas mixtures. *Proceedings of the Royal Society of London Series a - Mathematical and Physical Sciences*, 169(939):573–586.
- Hites, R. A. and Raff, J. D. (2012). *Elements of Environmental Chemistry*. John Wiley & Sons, second edition.
- Hoehn, E. and Cirpka, O. A. (2006). Assessing residence times of hyporheic ground water in two alluvial flood plains of the Southern Alps using water temperature and tracers. *Hydrology and Earth System Sciences*, 10(4):553–563.
- Hoehn, E. and von Gunten, H. R. (1989). Radon in groundwater - a tool to assess infiltration from surface waters to aquifers. *Water Resources Research*, 25(8):1795–1803.

- Höhener, P. and Surbeck, H. (2004). Radon-222 as a tracer for nonaqueous phase liquid in the vadose zone: Experiments and analytical model. *Vadose Zone J*, 3(4):1276–1285.
- Hunkeler, D., Hoehn, E., Höhener, P., and Zeyer, J. (1997). Rn-222 as a partitioning tracer to detect diesel fuel contamination in aquifers: Laboratory study and field observations. *Environmental Science & Technology*, 31(11):3180–3187.
- Huxol, S., Brennwald, M. S., Hoehn, E., and Kipfer, R. (2012). On the fate of ^{220}Rn in soil material in dependence of water content: Implications from field and laboratory experiments. *Chemical Geology*, 298-299:116–122.
- Huxol, S., Brennwald, M. S., and Kipfer, R. (2013). Processes controlling ^{220}Rn concentrations in the gas and water phases of porous media. *Chemical Geology*, 335(0):87–92.
- Igarashi, G., Saeki, S., Takahata, N., Sumikawa, K., Tasaka, S., Sasaki, Y., Takahashi, M., and Sano, Y. (1995). Ground-Water Radon Anomaly Before the Kobe Earthquake in Japan. *Science*, 269(5220):60–61.
- Inan, S. and Seyis, C. (2010). Soil radon observations as possible earthquake precursors in Turkey. *Acta Geophysica*, 58(5):828–837.
- Ivanovich, M. and Harmon, R. S. (1982). *Uranium series disequilibrium: applications to environmental problems*. Clarendon Press.
- Jury, W. and Horton, R. (2004). *Soil physics*. John Wiley, 6 edition.
- Kluge, T., Ilmberger, J., von Rohden, C., and Aeschbach-Hertig, W. (2007). Tracing and quantifying groundwater inflow into lakes using a simple method for radon-222 analysis. *Hydrology and Earth System Sciences*, 11(5):1621–1631.
- Krishnaswami, S., Graustein, W. C., Turekian, K. K., and Dowd, J. F. (1982). Radium, thorium and radioactive lead isotopes in groundwaters: Application to the in situ determination of adsorption-desorption rate constants and retardation factors. *Water Resour. Res.*, 18(6):1663–1675.
- Lane-Smith, D. (2009). personal communication.
- Langmuir, D. and Herman, J. S. (1980). The mobility of thorium in natural waters at low temperatures. *Geochimica et Cosmochimica Acta*, 44(11):1753–1766.
- Langmuir, D. and Riese, A. C. (1985). The thermodynamic properties of radium. *Geochimica et Cosmochimica Acta*, 49(7):1593–1601.

- Lehmann, B. E., Lehmann, M., Neftel, A., Gut, A., and Tarakanov, S. V. (1999). Radon-220 calibration of near-surface turbulent gas transport. *Geophysical Research Letters*, 26(5):607–610.
- Lehmann, B. E., Lehmann, M., Neftel, A., and Tarakanov, S. V. (2000). Radon-222 monitoring of soil diffusivity. *Geophysical Research Letters*, 27(23):3917–3920.
- Lehmann, B. E., Neftel, A., and Tarakanov, S. V. (2001). Continuous on-line calibration of diffusive soil-atmosphere trace gas transport using vertical Rn-220- and Rn-222-activity profiles. *Radiochimica Acta*, 89(11-12):839–843.
- Magill, J. and Galy, J. (2005). *Radioactivity Radionuclides Radiation*. Springer, Berlin Heidelberg.
- Mullinger, N. J., Binley, A. M., Pates, J. M., and Crook, N. P. (2007). Radon in chalk streams: Spatial and temporal variation of groundwater sources in the Pang and Lambourn catchments, UK. *Journal of Hydrology*, 339(3-4):172–182.
- Nagy, K., Berhás, I., Kovács, T., Kávási, N., Somlai, J., Kovács, L., Barna, I., and Bender, T. (2009). Study on endocronological effects of radon speleotherapy on respiratory diseases. *International Journal of Radiation Biology*, 85(3):281–290.
- Nazaroff, W. W. (1992). Radon transport from soil to air. *Reviews of Geophysics*, 30(2):137–160.
- Peterson, R. N., Santos, I. R., and Burnett, W. C. (2010). Evaluating groundwater discharge to tidal rivers based on a Rn-222 time-series approach. *Estuarine, Coastal and Shelf Science*, 86(2):165–178.
- Porcelli, D. and Swarzenski, P. W. (2003). The behavior of U- and Th-series nuclides in groundwater. In Bourdon, B., Henderson, G. M., Lundstrom, C. C., and Turner, S. P., editors, *Uranium-Series Geochemistry (Reviews in mineralogy and geochemistry)*, volume 52, pages 317–362. Mineralogical Society of America.
- Quattrocchi, F., Pik, R., Pizzino, L., Guerra, M., Scarlato, P., Angelone, M., Barbieri, M., Conti, A., Marty, B., Sacchi, E., Zuppi, G. M., and Lombardi, S. (2000). Geochemical changes at the Bagni di Triponzo thermal spring during the Umbria-Marche 1997-1998 seismic sequence. *Journal of Seismology*, 4(4):567–587.

- Rama and Moore, W. S. (1984). Mechanism of transport of U-Th series radioisotopes from solids into ground water. *Geochimica et Cosmochimica Acta*, 48(2):395–399.
- Ramsay, W. and Collie, J. (1904). The spectrum of the Radium Emanation. *Proceedings of the Royal Society of London*, 488-496:470–476.
- Ramsay, W. and Gray, R. (1910). La densité de l'emanation du radium. *Comptes rendus hebdomadaires des séances de l'Académie des sciences*, 151:126–128.
- Rogers, V. C. and Nielson, K. K. (1991). Correlations for predicting air permeabilities and ^{220}Rn diffusion coefficients of soils. *Health Physics*, 61(2):225–230.
- Rutherford, E. (1900). A radioactive substance emitted from thorium compounds. *Philosophical Magazine*, 49:1–14.
- Santos, I. R., Burnett, W. C., Chanton, J., Dimova, N., and Peterson, R. N. (2009). Land or ocean?: Assessing the driving forces of submarine groundwater discharge at a coastal site in the Gulf of Mexico. *Journal of Geophysical Research-Oceans*, 114.
- Scanlon, B., Massmann, J., and Nicot, J. P. (2002). Soil gas movement in unsaturated systems. In Warrick, A. W., editor, *Soil Physics Companion*, pages 297–341. CRC Press, Boca Raton.
- Schery, S. D., Gaeddert, D. H., and Wilkening, M. H. (1984). Factors affecting exhalation of radon from a gravelly sandy loam. *Journal of Geophysical Research-Atmospheres*, 89(ND5):7299–7309.
- Schmidt, A., Gibson, J. J., Santos, I. R., Schubert, M., Tattrie, K., and Wei, H. (2010). The contribution of groundwater discharge to the overall water budget of two typical boreal lakes in Alberta/Canada estimated from a radon mass balance. *Hydrology and Earth System Sciences*, 14(1):79–89.
- Schmidt, M., Graul, R., Sartorius, H., and Levin, I. (1996). Carbon dioxide and methane in continental Europe: a climatology, and ^{222}Rn -based emission estimates. *Tellus Series B-Chemical and Physical Meteorology*, 48(4):457–473.
- Schroth, M. H., Eugster, W., Gomez, K. E., Gonzalez-Gil, G., Niklaus, P. A., and Oester, P. (2012). Above- and below-ground methane fluxes and methanotrophic activity in a landfill-cover soil. *Waste Management (New York, N.Y.)*, 32(5):879–89.

- Schubert, M., Freyer, K., Treutler, H.-C., and Weiß, H. (2001). Using the soil gas radon as an indicator for ground contamination by non-aqueous phase-liquids. *Journal of Soils and Sediments*, 1(4):217–222. 1439-0108.
- Schubert, M., Paschke, A., Lau, S., Geyer, W., and Knöller, K. (2007). Radon as a naturally occurring tracer for the assessment of residual NAPL contamination of aquifers. *Environmental Pollution*, 145(3):920–927.
- Schubert, M., Schmidt, A., Paschke, A., Lopez, A., and Balczar, M. (2008). In situ determination of radon in surface water bodies by means of a hydrophobic membrane tubing. *Radiation Measurements*, 43(1):111–120.
- Sesana, L., Barbieri, L., Facchini, U., and Marcazzan, G. (1998). ^{222}Rn as a tracer of atmospheric motions: A study in Milan. *Radiation Protection Dosimetry*, 78(1):65–72.
- Sun, H. and Furbish, D. J. (1995). Moisture content effect on radon emanation in porous media. *Journal of Contaminant Hydrology*, 18(3):239–255.
- Sun, Y. and Torgersen, T. (1998). The effects of water content and Mn-fibe surface conditions on Ra-224 measurement by Rn-220 emanation. *Marine Chemistry*, 62(3-4):299–306.
- Surbeck, H. (1996). A radon-in-water monitor based on fast gas transfer membranes. In *Int. Conf. on Technologically enhanced Natural Radioactivity (TENR) caused by Non-Uranium Mining*, Szczyrk, Poland.
- Tanner, A. B. (1964). Radon migration in the ground: a review. In Adams, J. A. S. and Lowder, W. M., editors, *The Natural Radiation Environment*, chapter 21, pages 161–190. Univ. Press, Chicago.
- Tanner, A. B. (1980). Radon migration in the ground: a supplementary review. In Gesell, T. F. and Lowder, W., editors, *Natural Radiation Environment III*, volume 1, pages 5–56. US Dep. Energy. Rep. Conf. 780422, Washington.
- Tuller, M. and Or, D. (2005). Water retention and characteristic curve. In Hillel, D., editor, *Encyclopedia of Soils in the Environment*, pages 437–442. Elsevier Science, Oxford.
- Uchida, M., Nojiri, Y., Saigusa, N., and Oikawa, T. (1997). Calculation of CO_2 flu from forest soil using ^{222}Rn calibrated method. *Agricultural and Forest Meteorology*, 87(4):301–311.
- Valentine, R. L. and Stearns, S. W. (1994). Radon release from water distribution-system deposits. *Environmental Science & Technology*, 28(3):534–537.

Van Der Spoel, W. H., Van Der Graaf, E. R., and De Meijer, R. J. (1997). Diffusive transport of radon in a homogeneous column of dry sand. *Health Physics*, 72(5):766–778.

Corrigendum

Chapter 3

Section 3.3, page 25: "Under such "wet" conditions, the transfer of the radon gas molecules from the grains into the soil gas..." is replaced by
"Under such "wet" conditions, the transfer of radon nuclides from the grains into the soil gas..."

Section 3.4, page 27: "As the exact volume of the vessel could not be determined we use..." is replaced by:
"In every experiment, the exact air volume in the vessel was different due to the different subjects placed into the vessel. Therefore, we use..."

Section 3.5.1, page 28, caption of Figure 3.4: "Activity of the monazite pebbles..." is replaced by:
"²²⁰Rn-activity in air produced by the monazite pebbles..."

Section 3.5.1, page 29, caption of Figure 3.5: "Activity of the Mn-sand..." is replaced by:
"²²⁰Rn-activity in air produced by the Mn-sand..."

Chapter 4

Section 4.2.1, page 40: "The manganese sand was previously used in a technical application to scavenge radium from mineral water." is replaced by:
"The manganese sand was previously used in a technical application to scavenge manganese and radium from mineral water."

Section 4.2.1, page 40: "The total weight-specific ²²⁸Ra-activity (air dry) of the sand is 281±19 Bq/kg, determined by gamma-ray analysis using a germanium well detector." is replaced by:

“The total weight-specific ^{228}Ra -activity (air dry) of the sand is $281 \pm 19 \text{ Bq/kg}$, determined by gamma-ray analysis of the ^{228}Ac -activity using a germanium well detector.”.

Curriculum Vitae

Stephan Huxol

19. Februar 1981	Born in Münster/Westfalen, Germany
1987 - 1989	Primary school in Paderborn
1989 - 2000	Rudolf-Steiner School Schloss Hamborn School-leaving exam (Abitur)
2000 - 2001	Civil service
2001 - 2002	Studies in Physics University of Freiburg i. Brsg., Germany
2002 - 2007	Studies in Hydrology University of Freiburg i. Brsg., Germany
11/2007	Diploma in Hydrology
2007 - 2008	Scientific Assistant Institute of Hydrology, University of Freiburg i. Brsg., Germany
2008 - 2012	PhD student and research assistant in the Department of Environmental Systems Science of the Swiss Federal Institute of Technology Zürich (ETH) and in the De- partment of Water Resources and Drinking Water of the Swiss Federal Institute of Aquatic Science and Technol- ogy (Eawag), Dübendorf